MODELING OF A REAL TIME LEAK DETECTION SYSTEM IN PIPELINES

BY
AMIT KR. SINGH

GUIDED BY
Mr. DEEPAK DHARMARHA
Sr. MANAGER (PIPELINE DEPARTMENT)
ENGINEERS INDIA LIMITED

A report submitted in partial fulfillment of the requirements for Masters of Technology (Gas Engineering) of University of Petroleum and Energy Studies, INDIA

College of Engineering Studies
University of Petroleum and Energy Studies, INDIA
Village Bidholi, Near PremNagar
Dehradun.

DECLARATION

This is to certify that the dissertation report on "**MODELING OF A REAL TIME LEAK DETECTION SYSTEM**",submitted to University Of Petroleum And Energy Studies ,Dehradun ,India by **Mr. Amit Kr Singh** ,in partial fulfillment of the requirement for the award of degree of **Master Of Technology in Gas Engineering** ,is a bonafide work carried out by him under my supervision and guidance. The work has not been submitted anywhere else for any other degree.

Dr. D. N. Saraf
Distinguished Professor
College Of Engineering
U.P.E.S.,Dehradun

Dr. B. P. Pandey
Dean
College Of Engineering
U.P.E.S.,Dehradun

Acknowledgement

This is to acknowledge with thanks the help, guidance and support that I have received during the training.

I have no words to express a deep sense of guidance to the management of *Engineers India Limited* for giving me an opportunity to pursue my internship and in particular *Mr. A. Soni (H.O.D Pipeline)* and *Mr. Deepak Dharmarha (SR MGR.)* for their able guidance and support.

I must also thank *Mr. Ashok Singh, Mr. Pankaj Gupta* for their valuable support.

I also place on record my appreciation of the support provided by staff of various Departments of EIL.

AMIT KR .SINGH

M.Tech (Gas Engineering)
University of Petroleum
And Energy Studies
Dehradun.

Contents

A. OVERVIEW OF LEAK DETECTION

The methodologies used for leak detection cover a wide spectrum of technologies and processes and are based on a number of different detection principles. They vary from intermittent aerial inspections to hydrocarbon sensors to sophisticated real-time monitoring. Each approach has its strengths and weaknesses. These strengths and weaknesses are dependent on the application and the complexity of the pipeline system to which the leak detection is applied. In combination with processes and procedures, applying the appropriate technology (or technologies) is the key to an effective leak detection system.

Classification of Leak Detection Technologies

Leak detection technologies can be classified according to the physical principles involved in the leak detection. Using this type of classification, leak detection systems can be divided into the following four groups:

1. **Physical Inspection** - This type of leak detection involves either direct or remote visual inspection to detect a leak.

2. **Manual Tabulation** - This type of leak detection includes direct monitoring of pipeline flow and/or pressure for evidence of a leak. This may also involve manual calculations to identify lost product.

3. **Discrete Sensor-Based Technologies** - Sensor-based technologies rely on the use of an external sensor to detect the escaping hydrocarbon liquid. These systems include, but are not limited to:
- Liquid Sensing
- Vapor Sensing
- Acoustic emissions

4. **Computational Pipeline Monitoring** - Computational Pipeline Monitoring (CPM) systems are distinguished from other leak detection systems by the use of an algorithm that uses input from field sensors that monitor the internal pipeline parameters (e.g. pressure, flow, temperature, frictional pressure drop, density, batch interfaces) to determine when a leak has occurred. These systems include, but are not limited to:
- Over and short comparison
- Mass balance with line pack correction:

- Line pack correction based on pressure and temperature sensors
- Line pack correction based on transient flow modeling

- Pattern of discrepancy in pressure/flow between model and measurement
- Rate of pressure/flow change
- Statistical methods those are not model-based

• System identification methods based on digital signal analysis The operational principle, data and equipment requirements, the strength, the weakness, and the realistic performance limits (size, response time, location, false alarm) for leak detection methods listed above are addressed in the subsequent sections of this report.

Evaluation of Leak Detection Systems

Each leak detection system is unique based on the pipeline on which it is used. As such, the capabilities of the system and the degree to which it mitigates risk to high consequence areas (HCAs) must be evaluated for each pipeline system. More sophisticated systems will have more unique capabilities. The criteria used to evaluate the capability of an installed leak detection technology may include, but are not limited to, the following:

1. Leak Size or Leak Flow Rate - What is the minimum leak size that the system is capable of detecting? A leak is detectable only when its' effect rises above uncertainties in the variables being monitored (see Response Time below). The size of a leak is usually expressed as a percentage of the throughput of the pipeline. Leak size is a function of the size and shape of the opening (leak area) and the pipeline pressure. A leak can be either constant in size, such as a pre-existing small leak, or variable over time, such as a sizable leak that diminishes as the pipeline is depressurized.

2. Response Time - What is the time needed to detect a leak of a given size? Depending on the leak detection methodology used, the response time can vary over a wide range. For algorithms based on volumetric balance, the response time is related to the leak size. This is because of the uncertainties in the variables involved. Uncertainties, or noise in the variables used for leak detection, are always present. A leak can be detected only when its effect, herein called leak signal, is discernable amongst noise. Since noise is random in nature while a leak signal is not, over time, the accumulated noise remains at a noise level while the accumulated leak signal grows in size. Eventually, the accumulated leak signal rises above the noise and becomes detectable in a probabilistic sense (see False Alarms and Misses below). A minimum time period exists for each minimum detectable leak. A curve that relates minimum detectable leak size to response time is a leak threshold curve for this leak detection methodology. Two such leak threshold curves are shown in figure 2-1 to illustrate the general trend. Given an uncertainty level, larger minimum detectable leaks have a shorter response time. A smaller uncertainty in the variable results in a tighter threshold. It takes less time to detect for a given size leaks if the uncertainty is reduced. Small leaks with size approaching the combined no repeatability of instrumentation has a very long response time. Such leaks can only be determined by physical observations. For leak detection methods based on discrepancy patterns generated from a real-time transient flow model, the response time is not a function of leak size. Instead, it is a function of the propagation speed (about 3000 to 4000 ft/s) of a pressure disturbance and the distance between the leak and the nearest pressure or flow sensors.

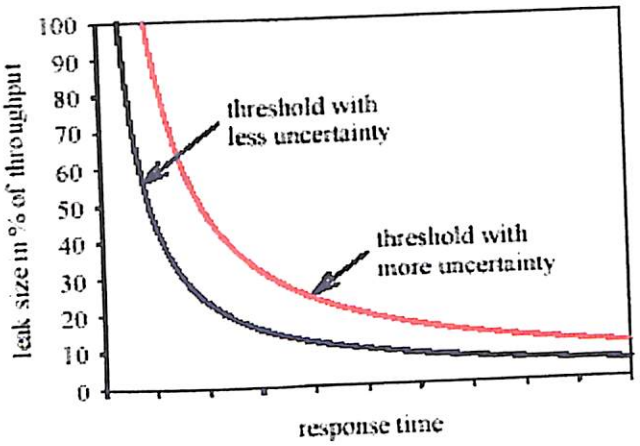

Figure 2-1 Detectable Leak Size Versus Response Time

3. Leak Location Estimation - Can the system locate a leak and what is the accuracy of the location estimate? The relevance of this criterion is to aid pipeline operator response to a leak in leak mitigation. Location can be estimated based on the time of arrival of a leak disturbance at a pair of sensors. Figure 2-2 indicates a leak occurring at time t0. This leak generates a local pressure drop, which then propagates both upstream and downstream. If this signal is picked up by pressure transducer A at time t1 and by pressure transducer B at time t2, then the leak can be located. This approach requires either a fast data scan rate or the time of arrival at the transducers is registered by data collectors and later transmitted to the control center.

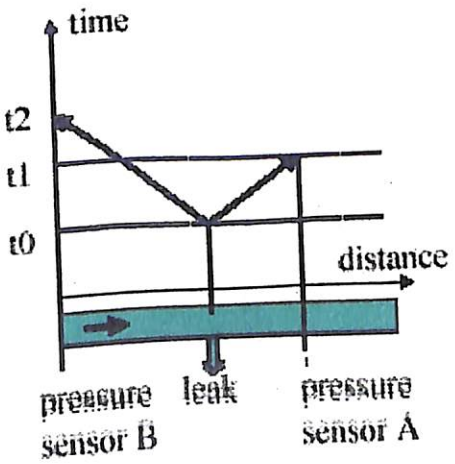

Figure 2-2 Locating a Leak by the Time of Arrival of a Leak Signal

Alternatively, a leak can be located by the profile of the piezometric head, also known as the hydraulic grade line. Figure 2-3 shows a pipeline with its inlet and outlet pressures held constant. The dotted profile is associated with the steady state flow prior to a leak. The solid profile is the hydraulic grade line after the transients caused by the leak have damped out and a new steady state is established. The leak steepness the upstream hydraulic grade and flattens the downstream hydraulic grade. The effectiveness of this approach relies on multiple pressure sensors along the pipeline so that segments of the hydraulic grade line can be defined after a leak has occurred

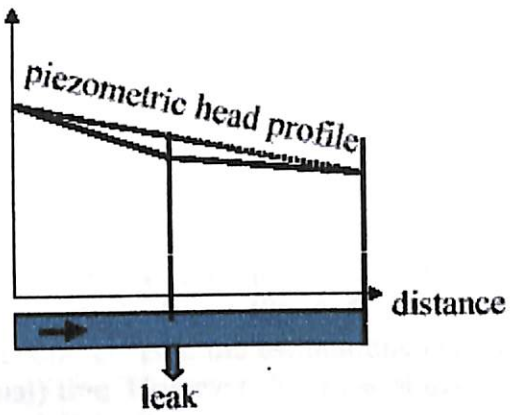

Figure 2-3 Locating a Leak by the Piezometric Head Profile

4. Release Volume Estimation - Does the system have the ability to determine the volume of liquid released? Reasonably accurate release volume estimation is possible for CPM methods where a mathematical model for transient flows is used. By using the measured pressure and flow from each end of a pipeline segment, the leak flow rate as a function of time can be calculated. Less accurate release volume can be estimated if a CPM method tracks the mean volume or mass imbalance (line fill change minus the difference between inflow and outflow). When a leak is detected, the volume or mass imbalance prior to and after the leak can be used to estimate the release volume over time.

5. Detecting Pre-existing Leaks - Does the system have the ability to detect between preexisting leaks, as well as, the onset of a new leak? Some CPM approaches depend on a change in one or several parameters to detect the onset of a leak. Such approaches will not be able to detect a leak (usually small) that is in existence before the CPM is activated.

6. Detecting a Leak in Shut-in Pipeline Segments - Does the system have the ability to detect the onset of a leak in a shut-in pipeline segment? The detection of a leak under such a situation is a matter of monitoring line fill change and discerning variations due to environmental temperature variations and/or due to a leak. CPM methods based only on metered inflow outflow comparison will not be able to detect a leak in a shut-in pipeline segment.

7. Detecting a Leak in Pipelines in a Slack Condition During Transients - Does the system have the ability to detect a leak in pipelines under a slack condition during transients? Liquid vaporizes when its pressure is sufficiently low. A pipeline is slack if vaporization occurs. A pipeline can be slack under both steady state and transient flow conditions. Leak detection on a slack line under transient conditions is difficult because the uncertainty in line pack change due to vaporization is large.

8. Rate of False Alarms and Misses - What is the false alarm rate for the system? There are many sources of uncertainty in the data that drive the CPM algorithm. These sources include hydraulic noise, non-repeatability of field sensors, uncertainties introduced by the data collection and communication system (analog-to-digital conversions, data timing), uncertainties in batch positions for product lines, and the state of flow (steady, drifting, or transient). As a result, the output from the algorithm is also uncertain. This uncertainty can be a significant issue facing the CPM technologies. To illustrate this issue, consider the volume imbalance as the algorithm output. In terms of standardized volumes, subtract the change of line fill over a time period from the difference between inflow volume and outflow volume over the same period. The result is the volume imbalance. A positive imbalance means a leak. Refer to Figure 2-4 where the estimated imbalance is plotted against the true imbalance. Had the estimations been perfect, all points should fall on the 45-degree (diagonal) line. However, because of uncertainties, the points will be scattered around the diagonal line. Points above the diagonal represent under-estimation of the imbalances, while points below the diagonal represent over-estimated imbalances.

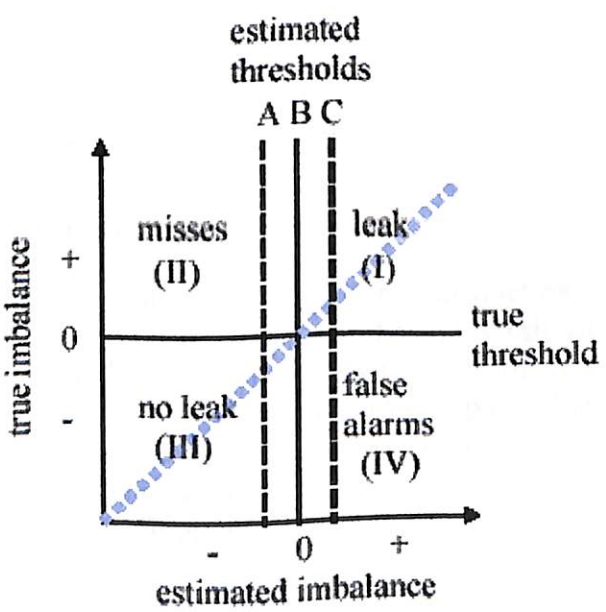

Figure 2-4 False Alarms, misses, and leak thresholds

The estimated imbalance versus true imbalance plot in Figure 2-4 is divided into four quadrants by the horizontal line labeled "true threshold" and the vertical line B that is the "perfectly estimated threshold." In reality, the true threshold is unknowable and the estimated threshold is determined empirically (by tuning, for example). Scatter of the points near the center of the plot gives rise to false alarms (for those points falling into quadrant IV) and misses (for those points falling into quadrant II). Notice that false alarms and misses occur even when the estimated threshold is perfect. For this reason, and given the fact that variable uncertainties are unavoidable, CPM is not the appropriate technology for detecting very small leaks. However, given the practical limitations of various other technologies, CPMs may be applied as long as their performance limitations are understood and acceptable to the pipeline operator. Given the scatter in the estimates, the frequency of false alarms can be reduced by raising the estimated threshold (vertical line C). In so doing, the chances of misses (leaks not detected) increase. Lowering the threshold (vertical line A) reduces the chances of misses at the expense of increasing the frequency of false alarms. Periods of greater line fill uncertainty occur when the pipeline is undergoing transients due to planned pipeline operations, such as pump startup and valve swings. To reduce the occurrence of false alarms, the leak threshold may be raised temporarily during such periods. Having the flexibility to raise the leak threshold can be an advantage, provided the operator understands that this is done at the expense of increased chances for misses (see Availability below).

9. Sensitivity to Flow Conditions - Will operational transients (such as those caused by pump startups or valve swings) degrade the ability to detect a leak? A pipeline seldom operates at a true steady state. This is especially true for long lines with numerous booster pump stations and delivery terminals. The line fill changes as a result of transients. Volume balance methods that do not compensate for line fill change accurately will be excessively sensitive to the flow conditions. The uncertainty in line fill induced by even mild transients can routinely exceed the combined non-repeatability of flow measurements in short time intervals. Transients generated by pump startups, shutdowns, and valve swings also put extra demands on the data collection system since data polling frequency and timing skew can become issues of concern. Shorter data sampling periods help to discern leaks in such a situation.

10. Robustness - Will degradation or malfunction of a system component cause catastrophic loss of leak detection ability? This criterion measures how gracefully the leak detection capability degrades when system components malfunction. It also measures a system's ability to function in complex pipeline configurations when not all the needed information is available. Pipeline operators should be alerted at the first sign of degradation so that restoration efforts can be initiated, and catastrophic loss of leak detection ability can be avoided.

11. System Self Check - Will the leak detection system have the capability to automatically check and possibly rectify parameters that affect leak detection performance? Will it have the capability to detect and locate non-functional or degrading field sensors and alert pipeline operators?

12. Ability to Handle Complex Pipeline Configurations - What is the ability of the system to handle complex pipeline configurations as well as complex operations? Complex systems may include multiple injection and delivery points, or multiple modes of operation. These may complicate CPM due to needed model (i.e. algorithm) refinements, increased data requirements, and increased uncertainty when the needed data is not available.

13. Availability - Is the leak detection algorithm active around the clock? To avoid false alarms, some CPM systems that can not handle transient flow conditions usually increase the detection threshold until the operational transients have passed. Since a leak is equally likely (or even more likely) to occur when a pipeline is an experiencing transient, the leak detection function is considered unavailable during periods of raised leak threshold. The percentage of time during which operational transients exist is an important factor in selecting the appropriate CPM method.

14. Retrofit Feasibility - What is required to install a new leak detection system and/or methodology on an existing pipeline? An upgrade requiring modification to or addition of, field sensors may be less feasible than one that only requires software modifications. Algorithms that require a prolonged period of on-line parameter tuning are more difficult to retrofit.

15. Ease of Testing - API 1130 "Computational Pipeline Monitoring" recommends that a leak detection system be tested during commissioning and every 5 years thereafter. As a result, ease of testing to affirm leak detection capability is a relevant criterion. Can the system be tested with pre-existing leak test data, as well as, by actual withdrawal?

16. Cost - What is the cost of the system including capital and operational expenses, as well as, data and equipment requirements?

17. Ease of Personnel Training - How are personnel trained on the operation and maintenance of the system? Is the system easy to operate? Complex systems requiring a high level of training may not afford the same level of leak detection capability when the human interface is considered.

18. Ease of Maintenance - What are the maintenance requirements for the system? Will the system degrade with improper or missed maintenance tasks?

Standards for Leak Detection Systems

Several industry consensus standards have been developed to address the selection, design, operation, and maintenance of leak detection systems. These standards include:

Table 2-1 Industry Leak Detection Standards

Standard	Revision	Title
API 1130	Second Edition November 2002	Computational Pipeline Monitoring
API 1149	November 1993	Pipeline Variable Uncertainties and Their Effects on Leak Detectability
API 1155	First Edition February 1995	Evaluation Methodology for Software Based Leak Detection Systems
API 1160	First Edition November 2001	Managing System Integrity for Hazardous Liquid Pipelines

Of the consensus standards, API 1130 has been incorporated by reference into 49 CFR 195. Specifically, section 195.134, "CPM leak detection" under Subpart C - Design Requirements, states:

"This section applies to each hazardous liquid pipeline transporting liquid in single phase (without gas in the liquid). On such systems, each new computational pipeline monitoring (CPM) leak detection system and each replaced component of an existing CPM system must comply with section 4.2 of API 1130 in its design and with any other design criteria addressed in API 1130 for components of the CPM leak detection system."

Section 195.444, "CPM leak detection" under Subpart F - Operation and Maintenance Requirements, states:

"Each computational pipeline monitoring (CPM) leak detection system installed on a hazardous liquid pipeline transporting liquid in single phase (without gas in the liquid) must comply with API 1130 in operating, maintaining, testing, record keeping, and dispatcher training of the system."

For the purpose of the regulations 49 CFR 195.2, "Definitions" defines CPM as follows:

"Computation Pipeline Monitoring (CPM) means a software-based monitoring tool that alerts the pipeline dispatcher of a possible pipeline operating anomaly that may be indicative of a commodity release."

B.
PROBABILISTIC LEAK DETECTION IN PIPELINES USING THE MASS IMBALANCE APPROACH

Typically, models of pipelines and pipe networks are calibrated to metered data by optimizing the choice of parameters according to some penalty function. This approach does not provide a natural way to assess the predictive uncertainty when these models are used to infer the presence and description of a leak. This report describes a fully probabilistic approach in which the activities of calibration and prediction are unified, using the mass-imbalance approach to leak detection as an example. The resulting probability distribution over leak location and size can be presented graphically, or it can be used within an optimal decision framework to compute an effective response taking uncertainty into account. The approach is generalized to different leak-scenarios, including multiple leaks.

Keywords: BAYESIAN, FRICTION FACTOR, RANDOM FIELD, CALIBRATION, CALIBRATED PREDICTION

1 INTRODUCTION

The development of methods for the detection of leaks in pipelines and pipe networks continues to be a very active research area (see, e.g., Mays, 1989; Pesta and Cassley, 1992; Mears, 1993; Mukherjee and Narasimhan, 1996; Rajtar and Muthiah, 1997, and the references below). Many proposals have the same underlying structure: to solve an inverse problem subject to parametric uncertainty and measurement error. The accepted approach appears to be to formulate the problem as an optimization. Kapelan et al. (2003a) provides a recent example (see also Purdar and Liggett, 1992; Kapelan et al., 2003b, and the references therein). In this report a model of a pipe network is parameterized by leak coefficients at each node and by Weisbach friction factors for each leg. Pressure observations are supplied for a subset of the nodes, and the sum of the squared differences between the observations and the physical model output is minimized over the possible values of the parameters. The result is a point estimate for the friction factors and the leak coefficients. In general a great deal of ingenuity is required to make this problem solvable in a practical sense, allowing that the optimand may be a rather irregular function of the parameters. For example, Kapelan et al. (2003a) propose a hybrid method combining the traditional Gauss-Newton approach with genetic algorithms.

It is not hard to see the deficiency in optimization approach, even in the cases where sufficient resources are available to ensure that a solution is found and that solution is indeed a global optimum in the parameter space. The point estimate conveys no measure of uncertainty. While there are generalizations that use the curvature of the optimand to infer a variance matrix (following a maximum likelihood approach), this type of approximation is only valid in the presence of large amounts of effectively-independent data: something that is seldom the case in the case of pipelines or pipe networks.

We need, however, to make a careful appraisal of uncertainty, because the detection of a leak is only the first stage in a complex decision about how to proceed. Decisions of this nature, i.e. potentially costly decisions made under uncertainty, are best approached within a decision theoretic framework in which actions are selected based on both probabilities and consequences (see, e.g., Lindley, 1985; Clemen, 1996; Bernado and Smith, 1994). What we would really like to compute in this situation is a joint probability distribution over leak location and size, taking account of parametric uncertainty and measurement errors, and also taking account of expert knowledge about the ways in which the particular pipe network might leak.

It may be argued that the probabilistic approach is simply too difficult, and the formulation of the leak detection problem as an optimization is a practical compromise although, interestingly, this point is seldom made explicitly. This paper seeks to challenge this view, demonstrating how a simple leak detection approach the mass imbalance method can be made fully probabilistic, and showing the kinds of results that

can then be derived. The mass-imbalance approach is used because its simplicity lends itself to a clear exposition of the key features of the probabilistic approach, but it should be clear that the method could be extended immediately to more complex systems such as pipe networks.

The key point of this report is that the probabilistic approach is a natural generalization of the optimization approach, or, to put it another way, the optimization approach is actually the probabilistic approach but with very strong (and, one might add, unrealistic) assumptions about the distributions of the uncertain quantities. Therefore methods that are currently formulated as optimizations can be made probabilistic quite straightforwardly, and, if necessary, in stages. Powerful computers and recent advances in inferential calculations, such as Markov chain Monte Carlo sampling , have helped to make fast probabilistic inference possible. These types of stochastic techniques can be improved by a first-stage optimization in order to select an efficient proposal distribution, which is another way in which the probabilistic approach can be seen as a generalization of the optimization one.

The outline of the report is it describes the steady state behaviour of a pipeline with a leak, and the deterministic mass imbalance leak location method; a full list of notation used in this and subsequent sections is given at the end of the report. It describes the sources of uncertainty, and how they may be accommodated within a probabilistic approach to leak description using the mass imbalance method. This includes a demonstration of two ways in which the probabilistic approach can be used to generalize the deterministic one. The report describes how we might describe the engineer's knowledge about the Weisbach friction factor, which is often the major contributor to parametric uncertainty. This is treated as an uncertain function, or random field, along the pipeline. It provides a simple example, demonstrating one way in which probabilistic information about leak location and leak size may be presented. This also illustrates that reasonable choice for the distributions of the unknown parameters can give rise to a large amount of uncertainty about the leak. It generalizes the probabilistic model used to describe the engineer's knowledge about the ways in which the pipeline might leak, to encompass leak detection and leak attribution.

The steady state equation for a non-leaking pipeline is

$$H - \frac{\rho(L)}{D}\frac{v^2}{2g} - \kappa\frac{v^2}{2g} = 0 \qquad \textbf{(1a)}$$

where H is the upstream piezometric head, L and D the pipeline length and pipe diameter, v the velocity (assumed to be positive), g the gravitational acceleration, the downstream valve coefficient, and

$$\rho(x) \triangleq \int_0^x f(z)\,dz \qquad (1b)$$

Where f(x) is the Weisbach friction factor at location $x \in [0, L]$. This friction factor is allowed to be non-constant along the pipeline, according to variations in pipe roughness. In (1a) the first term H is the total head available, and the second and third terms describe how that head is dispersed by friction along the pipeline, and by the valve at the downstream end of the pipeline. Details may be found in, e.g., Massey (1989) or Wylie and Streeter (1993). Eq. (1) is one of the simplest configurations of a pipeline, in terms of its boundary conditions and its lack of features such as additional valves, or constrictions such as bends or variations in pipe diameter. This simplicity aids presentation, but it is not a restriction on the application of the probabilistic approach described below. The probabilistic approach can be generalized in exactly the same way as the physical model, since it sits 'on top' of the physical model.

If we introduce a single leak at location $\ell \in (0, L)$, then we can describe the loss of liquid through the leak with an orifice equation

$$v_0 - v_L = \gamma\sqrt{2gh(\ell)} \qquad (2a)$$

Where v_0 and v_L are velocities at the upstream and downstream ends of the pipeline, γ is a lumped coefficient representing leak size and discharge coefficient, and $h(\ell)$ is the piezometric head at the leak location. The steady state equation is now

$$\underbrace{H - \frac{\rho(\ell)}{D}\frac{v_0^2}{2g}}_{h(\ell)} - \frac{\rho(L) - \rho(\ell)}{D}\frac{v_L^2}{2g} - \kappa\frac{v_L^2}{2g} = 0 \qquad (2b)$$

Where the second and third terms represent the head dispersed by friction above and below the leak at ℓ, and $h(\ell)$ is indicated. The friction factor is taken to be invariant to the changes in fluid velocity that follow the onset of the leak. In other words velocity is sufficiently high or the pipe sufficiently rough that the flow is fully turbulent, to the extent that even a large leak does not affect the Reynolds's number sufficiently to impact on the friction factor. Alternatively, we could restrict attention to small leaks, for which v_0 and v_L remain close to v, the pre-leak velocity.

Taken together, (2) gives us three equations in the three unknowns v0, vL and $h(\ell)$. If we had precise values for the other parameters, we could solve for these unknowns exactly. For leak detection, however, we need to solve a different problem, because the leak is the unknown. This report considers the mass imbalance approach , in which we infer the leak location from information about v0 and vL. With these two data we can solve (2b) for $\rho(\ell)$, which we can then invert to find ℓ, since $\rho(\cdot)$ is continuous and strictly increasing. The key question is how best to proceed when we do not have precise values of the other parameters. In the next section we treat this question in terms of probabilities.

2 INFERENTIAL CALCULATIONS

2.1 SOURCES OF UNCERTAINTY

There are three sources of uncertainty when applying the mass imbalance approach. First, measurement uncertainty. The values v0 and vL are not necessarily the true steady-state velocity values, owing to transient fluctuations in the fluid, and to measurement errors. The same could be said for the piezometric head H, but in this report we are treating this as known, for simplicity. We can remove the effect of transient fluctuations by time-averaging, because transient behavior in an incompressible fluid tends to die away rapidly. This assumption is common in steady-state methods (Mukherjee and Arasimhan, 1996). However, the restriction to steady state is not a necessary condition for a probabilistic treatment: Rougier and Goldstein (2001) derive a fully-probabilistic treatment of transient fluid behavior, useful in situations where the boundary conditions are constantly changing, or where the transients reflect extreme events like rapid valve closure. Removing transient effects leaves systematic meter bias as the main source of measurement uncertainty, for example mis-calibration or externally driven bias such as the effects of changes in ambient temperature. These tend to vary slowly in time to the extent that they can be treated as unknown constants for real-time monitoring.

The second source of uncertainty is parametric uncertainty. At any point in time we may not know the exact setting of, say, the downstream valve. More generally, we cannot ever know the function $\rho(\cdot)$, which is effectively an infinite dimensional parameter (i.e. one for which no finite set of measurements will ever be sufficient). Furthermore, we seldom know, before the event, the location and size of the leak, should one occur.

The third source of uncertainty is model uncertainty, also termed model inadequacy. Our model, described by (1) in the absence of a leak, is not a perfect analogue for the underlying pipeline. To put this more formally, we cannot imagine making precise measurements of the parameters with the property that the model evaluated at those parameters would give an exact match with precise measurements of pressure and flow. To give one example, we do not know how to make a precise measurement of the 'relative roughness' of a pipe, which is an abstraction of a much more complex phenomenon.

The treatment of model inadequacy is a rapidly developing area in statistics (see, e.g., Kennedy and O'Hagan, 2001; Craig et al., 2001; Goldstein and Rougier, 2004; Higdon et al., 2004), with direct implications for both model calibration and prediction. The simplest approach, which we will adopt here for convenience, is to accept the strong constraint. This states that although we know our model to be imperfect, we still believe that somewhere in the parameter space there is a combination of values that would make our model a perfect match for the pipeline itself. This is consistent with optimization approaches to calibration, which are prevalent in leak detection, as discussed in the Introduction. The less restrictive model, sometimes referred to as the best-input model (Rougier, 2004), is a straightforward generalization that can be added into the probabilistic approach below, when the strong constraint is deemed inappropriate.

2.2 THE PROBABILISTIC MASS IMBALANCE APPROACH

We recast the mass imbalance approach in probabilistic terms. The task is to infer the distribution of leak location ℓ and leak coefficient γ conditional on imperfect observations of the upstream and downstream velocities, and taking account of our uncertainty about the valve coefficient κ and uncertainty about the friction factor, which leads to uncertainty about $\rho(\cdot)$.

The first point to note is that we if we have two velocity meters we should have more than two velocity observations: potentially we have four. Prior to the leak occurring we have the measurements v_0^0 and v_L^0 where the superscript '0' indicates that no leak has occurred. Since both velocities should be equal to v, any difference between them must be on account of systematic meter bias. Denote the biases as c_0 and c_L, so that $v_0^0 = v + c_0$ and $v_L^0 = v + c_L$. Then after the leak occurs we have two different measurements, but the same systematic biases. In other words, $v_0^1 = v_0 + c_0$ and $v_L^1 = v_L + c_L$ where the superscript '1' indicates the presence of a single leak. We can choose to disregard the measurements of v_0^0 and v_L^0 just as the deterministic mass imbalance approach does, but the probabilistic approach allows us to include these data, and we would expect them to be informative because they can help us to 'correct' our prediction to take account of meter bias.

In this subsection, however, we use only the post-leak values v_0^1 and v_L^1 to stay as close as possible to the deterministic mass-imbalance method, and to give the clearest possible explanation of the general probabilistic approach. In subsection 3.3 we generalize to include pre-leak values as well.

Our objective is to compute $\Pr(\theta, \gamma \mid v_0^1, v_L^1)$ where the observed values of random variables are denoted with an over bar. However, in order to make use of the physics in (2), we need to introduce additional uncertain quantities, namely $\rho(0)$, $\rho(L)$ and κ. For simplicity we eliminate h(l) using (2a) and (2b), to give

$$v_0 - v_L = \gamma\sqrt{2g\left(H - \frac{\rho(0)}{D}\frac{v_0^2}{2g}\right)}. \qquad (3)$$

Writing

$$\theta \triangleq (\ell, \gamma, \rho(0), \rho(L), \kappa), \quad v \triangleq (v_0, v_L), \quad \text{and } V \triangleq (v_0^1, v_L^1) \qquad (4)$$

For reasons that will be explained immediately below) the predictive Probability Density Function (PDF) becomes

$$\Pr(\theta, v \mid \bar{V}) = c\Pr(\theta, v, V = \bar{V}) = c\Pr(V = \bar{V} \mid \theta, v)\Pr(\theta, v) \qquad (5)$$

where

$c \triangleq \Pr(V = \bar{V})^{-1}$ and $\bar{V}$ are the observed values of V. The equivalence follows from the definition of conditional probability, and the following equality is a factorization of the joint distribution that is often referred to as Bayes's Theorem, the two PDFs being the likelihood function and the prior distribution, respectively. In practice we seldom need to compute the normalizing constant c explicitly, and so we can ignore it in what follows.

The problem is that (5) is not easily computable, because the likelihood function is regenerate: it is zero almost surely for reasonable choices of (θ, v) because when we put a choice in (2b) and (3) along with the two values in $\bar{V}$ these two equations will not hold simultaneously (technically they will hold only on a set of measure zero). This requires quite careful handling. We must choose two of our uncertain parameters to be constrained by the physical model and the data combined. The natural choices are the two values in, v because for given θ the two equations (2b) and (3) define a bi ejective mapping,

$$v = \cdot V. \qquad (6)$$

That is to say, if we are given θ and $\bar{V}$ we can solve for r and if we are given θ and r we can solve for V. This may not be obvious. The reason is that using θ we can solve (2b) and (3) for (v_0, v_L) Then we can either compute r using V, or $\bar{V}$ using r, since

$$\bar{V} = (v_0, v_L) + r. \qquad (7)$$

Denote by $\bar{r}$ the solution values for r using $\bar{V}$ at the given θ. The predictive distribution is not affected if we remove from the prior PDF regions of the parameter space with zero likelihood. Therefore we can express (5) as

$$\Pr(\theta \mid \bar{V}) = c \Pr(\bar{V} \mid \bar{V}, \theta, \bar{r}) \Pr(\theta) \qquad (8a)$$

where we have removed all non-compatible values of r by making r a deterministic function of θ and $\bar{V}$. Following on from (6), the event $(\bar{V} \mid \bar{V}, \theta, \bar{r})$ is equivalent to the event $(r = \bar{r} \mid \theta, \bar{V})$ Making this substitution, the resulting form for the predictive distribution

$$\Pr(\theta \mid \bar{V}) = c \Pr(r = \bar{r} \mid \theta, \bar{V}) \Pr(\theta). \qquad (8b)$$

If we want to simplify this further we have to make some additional choices about the marginal distribution of (θ, r). An obvious simplification presents itself: the engineer's knowledge about the meter biases is independent of his or her knowledge regarding the other uncertain quantities. Taking this to be acceptable, we can simplify the predictive distribution to

$$\Pr(\theta \mid \bar{V}) = c \Pr(r = \bar{r}) \Pr(\theta) \qquad (8c)$$

where it is understood that the value r is a function of θ and $\bar{V}$. In other words, the likelihood function for θ is constructed from the engineer's knowledge about the meter biases. Informally, the larger the biases are thought to be, the less informative the data in $\bar{V}$ will be about θ, where θ includes the leak's location ℓ and size coefficient κ.

Like the likelihood function, the prior distribution $\Pr(\theta)$ can also benefit from some quite natural simplifications. First, the engineer's knowledge about the friction function $f(\cdot)$ is very likely to be independent of his or her beliefs about the other uncertain quantities. Similarly, the engineer's knowledge about the valve coefficient κ is very likely to be independent of the other uncertain quantities. Finally, the engineer's knowledge about the

leak coefficient κ is very likely to be conditionally independent of the other uncertain quantities given the leak location, ℓ. If these are acceptable, we can write the prior distribution in (8c) as

$$\Pr(\theta) = \Pr(\ell, \kappa, p(0), p(L), \kappa)$$
$$= \Pr(p(0), p(L) \mid \ell) \Pr(\kappa \mid \ell) \Pr(\ell) \Pr(\kappa) . \qquad (9)$$

We are taking the pipeline length L as known throughout, so the first PDF represents the engineer's knowledge about $p(\cdot)$ at two known locations 0 and L. Note that the one dependence that has been preserved in (9) is that of leak size on leak location. This allows the engineer to incorporate the knowledge that leaks in certain locations are likely to be bigger than others, for example those that occur in regions of seismic activity. More details of this kind of statistical modeling are given in section 6. Using (8c) and (9), and specifications for the PDFs therein, we can turn the data V into a prediction for (ℓ, κ). using standard probabilistic tools such as Monte Carlo sampling.

Note that the probabilistic approach can go where the deterministic one cannot: leak location with a single meter. Suppose that we have just the downstream meter. Given θ, we still have a bijective mapping between q_L and v_L^1 and consequently we can compute q_L and the predictive distribution for θ becomes

$$\Pr(\theta \mid v_L^1) = c \Pr(q_L \mid q_L) \Pr(\theta) \qquad (10)$$

Where $c \triangleq \Pr(v_L^1 \mid v_L^1)^{-1}$, $\Pr(\theta)$ is as given in (9). The amount of information that the observation v_L^1 can contribute will depend strongly on the prior. For example, if $\Pr(\ell)$ consisted of two widely separated narrow peaks then we would expect v_L^1 to be highly informative, as it would typically select one peak or the other. On the other hand, if $\Pr(\ell)$ was at over the interval $(0, L)$ then we would expect that v_L^1 would not do much more than put a bulge or a tilt into the predictive distribution of ℓ.

2.3 USING PRE-LEAK MEASUREMENTS

We can follow the steps outlined in the previous section to incorporate the extra information available in the observations (v_0^0, v_L^0). We use the difference $v_0^0 - v_L^0 = q_0 - q_L$, and redefine the collection V as

$$V \triangleq (v_0^0 - v_L^0, v_0^1, v_L^1) \qquad (11)$$

We can write the relation between the observations V and the biases ε as

$$\begin{pmatrix} v_0^0 & v_L^0 \\ v_0^1 & \\ v_L^1 & \end{pmatrix} = \begin{pmatrix} 0 & 0 \\ 1 & 0 \\ 0 & 1 \end{pmatrix} \begin{pmatrix} \varepsilon_0 \\ \varepsilon_L \end{pmatrix} + \begin{pmatrix} 1 & 1 \\ 1 & 0 \\ 0 & 1 \end{pmatrix} \begin{pmatrix} \varepsilon_0 \\ \varepsilon_L \end{pmatrix}. \qquad (12)$$

As we can solve (2b) and (3) for $(\varepsilon_0, \varepsilon_L)$ using θ, we can map from ε to V given θ using (12). This mapping is not invertible, but we can use the structure of (2) that it is still possible to map back from V to ε. We can write the left-hand side of (2a) as

$$\begin{aligned} \varepsilon_0 - \varepsilon_L &= (v_0^1 - \varepsilon_0) - (v_L^1 - \varepsilon_L) \\ &= v_0^1 - v_L^1 - (\varepsilon_0 - \varepsilon_L) \\ &= v_0^1 - v_L^1 - (v_0^0 - v_L^0) \end{aligned} \qquad (13)$$

Which is a known value given V. Therefore we can solve (2a) directly for the value of h(l), which we can substitute into (2b) to solve for ε_L. Once we have solved for ε_L we can compute $\varepsilon_L - v_L^1 - v_L$ and then we can find $\varepsilon_0 = (v_0^0 - v_L^0) + \varepsilon_L$.

Therefore we have shown once again that given θ we have a bijective relationship

$$\varepsilon \leftrightarrow V. \qquad (14)$$

Where V is now the collection given in (11).

Therefore (8c) still holds under the new definition of $\bar{V}$ (being the observed values of the new V). The collection $\bar{\varepsilon}$ has the same meaning, namely those values that are implied by θ and $\bar{V}$, but the procedure for computing $\bar{\varepsilon}$ is different, and, in fact, simpler. No extra input is required of the engineer, so the incorporation of the extra datum $\bar{v}_0^0 \quad \bar{v}_L^0$ is genuinely a `free upgrade'.

2.4 LIKELIHOOD-BASED APPROACHES TO INFERENCE

It may be helpful to outline the statistical justification for the optimization approach so that we can see how it could be extended to include uncertainty assessments regarding the leak, and how this contrasts with probabilistic methods.

Optimization through minimizing a least-squares penalty function can be justified in inferential terms using maximum likelihood (see, e.g., Pawitan, 2001). In general, the Maximum Likelihood Estimator (MLE) $\hat{\theta}$ satisfies

$$\hat{\theta} \triangleq \max_{\theta} \Pr(r = \bar{r}) \qquad (15)$$

Remembering that $\bar{r}$ is a function of θ and $\bar{\Gamma}$. We must assume that the meter biases are gaussian, with known means and variances. Taking the means to be zero and denoting the variance matrix as Σ, the MLE is then

$$\hat{\theta} = \max_{\theta} \{ -\bar{r}^T \Sigma^{-1} \bar{r} \} \qquad (16)$$

Where $\bar{r}^T$ is the transpose of the vector $\bar{r}$. This is the (generalized) least square formulation. However, in order to make inferences about the leak, i.e. to have more than a point estimate for θ, we ought to compute not the MLE but the profile likelihood

$$L(\ell, \gamma) \triangleq \max_{\theta:\{\ell,\gamma\}} \Pr(r = \bar{r}) \qquad (17)$$

Using this profile likelihood we can calculate a value for the variance of our estimates for (ℓ, γ), although this calculation is not at all straightforward. The calculated value is asymptotically correct in the limit as the length of ε becomes large, and subject to conditions on the approximate independence of the components of ε. The problem is, however, that for leak detection the measurements are seldom abundant and often dependent. For the simple mass-imbalance approach, for example, we cannot feel confident about an asymptotically justified measure of uncertainty based on only two data. Therefore likelihood-based approaches would appear not to be particularly useful in determining our uncertainty about θ.

Once we move away from likelihood-based inference in our search for measures of uncertainty about the leak, it is natural first of all to consider the probabilistic case with a

prior distribution for θ, subject to limits on the values of each of the components. In this case we can treat the likelihood function as the predictive distribution, subject to renormalization. No new choices have to be made (except for the limits), but the treatment of the data is quite different. Rather than maximize the likelihood function for a point estimate of θ, we would now sample from it (as described in section 5), or summaries it directly by integrating over θ to find the mean vector and variance matrix.

But at this point we may well ask whether at prior for θ is really an adequate reflection of the engineer's knowledge about the pipeline. The fully probabilistic approach provides the engineer with an opportunity to incorporate his or her knowledge about the pipeline into the inferential calculation. The engineer can adopt or feign ignorance and stick with a prior, but this is a choice and not a mandatory part of the inferential process. For example, if some leaks are believed to be more likely than others, then this information can go into $p(\theta)$, likewise if some parts of the pipeline are believed likely to be rougher than others, or small values for the valve coefficient are believed to be more likely than large ones.

To summarize the argument in this subsection, the optimization-based approach to choosing a point value for θ does not generalize easily, if at all, to computing measures of uncertainty. If we want such measures then we have to adopt a fully probabilistic approach. Once we have made this step, the opportunity arises to incorporate the engineer's knowledge into the inferential process, which we expect to improve our assessment of θ to the extent that the engineer's knowledge about the pipeline is well founded.

3 MODELLING KNOWLEDGE ABOUT THE FRICTION FACTOR

The previous calculations involve the PDF of $p(\cdot)$ at given locations along the pipeline. The function $p(\cdot)$, defined in (1b) is uncertain because the Weisbach friction factor $f(\cdot)$ is uncertain. This section explains why f might be treated as uncertain, and how f can be modeled in a flexible manner so that the resulting solution remains tractable.

3.1 SOURCES OF UNCERTAINTY

The standard method to assess $f(\cdot)$ is to determine from experimental data the equivalent sand-roughness of the pipe material, and then to determine, by further experiment, the relation between equivalent sand-roughness and the friction coefficient. In practice it is uneconomical to perform these experiments, and so the results of standard experiments are used instead, in the form of tabulated values or mathematical formulae (see, e.g., Colebrook, 1939). The consensus, as summarized by Massey (1989, p. 204) is that accurate prediction of friction losses is thus difficult to achieve." As for the scale of the uncertainty, Haaland (1983, p. 90) notes that the Colebrook-White formula " . . . may be

3-5 percent, if not more, in error as compared to experimental data", on top of which should be added uncertainty about equivalent sand-roughness. As losses to friction will dominate the other losses in many pipelines, this seems to justify a careful stochastic analysis.

3.2 BELIEFS ABOUT THE FRICTION COEFFICIENT

The two requirements of a stochastic approach are (a) to find a way to model knowledge about the friction coefficient along the pipe, and then (b) to turn this into

$$\Pr(\mu(x_1), \ldots, \mu(x_n) \mid x_1, \ldots, x_n). \qquad (18)$$

Where (x_1 to x_n)are any finite set of locations along the pipeline. This latter PDF is required in the inferential calculations described in the previous section, for the special case$(x_1, x_2) = (\ell, L)$. But the more general treatment is useful in case we have access to pressure readings at known locations along the pipeline, which we would like to incorporate into our predictive distribution using the methods previously described.

The technical difficulties of part (b) will restrict the choices for part (a). In fact the only tractable and non-trivial model for the friction coefficient is a gaussian random field. This model is parameterized by a mean function $\mu_1(\,)$ and a covariance kernel $\mu_2(\,,\,)$:

$$\mu_1(x) \triangleq \mathrm{E}(f(x)), \quad \text{and} \quad \mu_2(x, x') \triangleq \mathrm{Cov}(f(x), f(x')). \qquad (19)$$

The mean function is the best guess for the point wise value of the friction factor along the pipeline (it may, for example, be a constant). The covariance kernel μ_2 describes two aspects of uncertainty about the difference between the actual friction factor and the mean value. First there is the point wise uncertainty, i.e. how far the true value might deviate from the mean value at each point. This is represented by the standard deviation$\sqrt{\mu_2(x, x)}$. Second, there is the degree to which deviations at different points are related, represented by the correlation$\mu_2(x, x')/\sqrt{\mu_2(x, x)\,\mu_2(x', x')}$. As we assume that f is a gaussian random field the joint distribution of any finite collection is gaussian. This is not ideal, as the gaussian distribution does not respect the constraint that f (x) > 0. However, it will usually be the case that Pr (f(x) <= 0) is tiny, in which case the implicit truncation of f(x) at zero will have no practical effect. The great practical advantage of using a gaussian random field is that it follows that (18) is also gaussian.

The mean and covariance of designated points on $\alpha(\cdot)$ are then given by

$$\begin{aligned} E(p(x) \mid x) &= \int_0^x \mu_1(z)\,dz, \text{ and} \\ \text{Cov}(p(x), p(x') \mid x, x') &= \int_0^x \int_0^{x'} \mu_2(z, z')\,dz'\,dz. \end{aligned} \tag{20}$$

3.3 CHOICES FOR THE COVARIANCE KERNEL

The simplest choice for $\mu_2(x, x')$ is $\mu_2(x, x') = 0$. This would be appropriate if there was complete certainty about the friction coefficient at every location along the pipe. The next simplest choice is $\mu_2(x, x') = \sigma^2$ for some known quantity σ. This would be appropriate if a single error-free measurement at any location in the pipe would be sufficient for complete knowledge at every point in the pipe. In other words, there is perfect correlation between f(x) and f (x') for all x and x'. These two choices would appear to be inappropriate for real-world pipes.

If knowing the friction coefficient at x was not sufficient for knowing the coefficient at some other location x' then the correlation between f (x) and f (x') would have to be less than one. If the point wise uncertainty was the same along the pipe and the correlation depended only on the separation between x and x' then the appropriate model would be a stationary kernel of the general form $\mu_2(x, x') = \sigma^2 r(x - x')$, where the function $r(\cdot)$ must be positive definite. Here σ describes the point wise uncertainty about the friction coefficient, while $r(\cdot)$ controls how the correlation between coefficients at two different locations drops according to their separation. Essentially, $r(\cdot)$ controls the predictability of f (x') from knowing the value f (x).

More general specifications for $\mu_2(x, x')$ are possible, in which the variance is not required to be the same at all, points but depend upon the location, and in which correlation as a function of distance also depends upon the location. These would be useful in the presence of detailed beliefs about the behavior of the friction coefficient along the pipe. The stationary case with appropriate selection of the function $r(\cdot)$ should be sufficiently flexible to model general uncertainty.

3.4 PRACTICAL ISSUES

In general the friction factor depends on both the equivalent sand-roughness and on the Reynolds number. In this paper, however, we restrict attention to the case where the pre-leak velocity is sufficiently large or the leak size sufficiently small that the friction factor both before and after the leak can be modeled with a constant known Reynolds number. Writing K (x) for the equivalent sand-roughness at location x and 'Re' for the Reynolds number, we can use the Colebrook-White formula.

$$\frac{1}{\sqrt{f(x)}} = -2\log_{10}\left(\frac{2.51}{Re\sqrt{f(x)}} + \frac{K(x)}{3.7D}\right) \qquad (21)$$

To induce uncertainty about f (x) from uncertainty about K (x). Unfortunately f (x) is not a linear transformation of K (x), and so we cannot assign a gaussian random field to $K(\cdot)$ and then infer the mean function and variance function for $f(\cdot)$ directly. However, we can use our point wise uncertainty about K (x) to induce point wise uncertainty about f (x). The simplest way to do this is by sampling K (x) and then summarizing the transformed values for f (x) in terms of the mean and standard deviation.

If we accept that a stationary random field is appropriate for $f(\cdot)$, then there is a natural choice for $r(\cdot)$, namely the Ornstein-Uhlenbeck correlation function

$$r(d) = \exp(-\tau d) \qquad (22)$$

For $\tau > 0$. This correlation function generates quite 'rough' sample paths (no pun intended) that are continuous but not differentiable in the mean-squared sense. It has the *markov* property that, for three locations x < x' < x",

$$Cov(f(x), f(x'') \mid f(x')) = 0.$$

In other words if we knew the friction coefficient at x' then also knowing the coefficient at x would be of no additional help in predicting the coefficient at x". This seems appropriate for pipelines, in which both the original pipe roughness and the subsequent internal surface degradation might be driven primarily by local factors. This correlation function also has the attractive feature that we can compute the covariance of $p(\cdot)$ directly:

$$Cov(p(x), p(x') \mid x, x') = (\sigma/\tau)^2(1 - e^{-\tau x'})(e^{\tau x} - 1) \qquad (23)$$

For $x' < x$. This explicit form for the covariance helps to speed up the inferential calculations because we need to compute $Cov(p(\ell), p(L) \mid \ell)$ for every candidate value for ℓ.

4 CALCULATIONS BASED ON MODEL

Consider the following example. Oil with kinematic viscosity $10^{-0.5}$ m^2/s flows through a cast-iron pipe D = 0:1m in diameter and L = 1000m long under a piezometric head difference of H = 50m, terminating at a valve.

4.1 SPECIFYING PRIOR KNOWLEDGE

In order to treat the leak detection probabilistically, we need to specify the engineer's prior knowledge about (a) the friction factor and the valve coefficient; (b) the likely location and size of the leak; and (c) the velocity meter accuracy. In this subsection we specify `reasonable' choices that may be applied across a range of actual problems.

The PDF of the friction factor is chosen using the approach described in section 4.4, based on knowledge about the relative roughness of cast iron. Before we do this we need a typical value for the velocity, to compute the Reynolds number. This can be found from (1) and (21), setting the valve coefficient and the equivalent sand-roughness to their best guess values, for which we choose 49 and 0.25* 10^{-3} m, respectively. This gives a velocity of 1.64 m/s, and a Reynolds number of 16.4 * 10^3. This combination of Reynolds number and relative roughness put the pipeline in the transition zone between laminar flow and complete turbulence.

Using this Reynolds number we can sample a large number of values for based on uncertainty about . We treat the marginal distribution of K (x) as invariant to x, and assign it a Gamma distribution. The Gamma distribution is a simple but flexible choice for strictly positive quantities; its PDF is given on next page

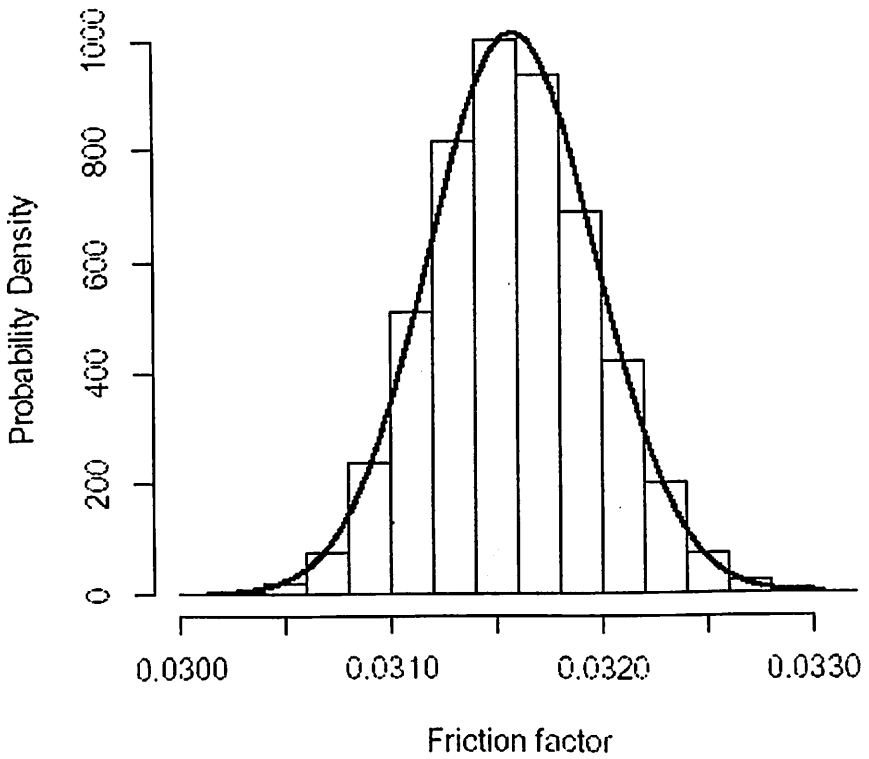

Figure 1: The marginal distribution of the Weisbach friction factor $f(x)$, based on uncertainty about the equivalent sand-roughness of cast iron. The overlaid curve shows a gaussian density function.

in eqrefeq:Gamma. For $K(\cdot)$ we choose a mean of 0:25 * 10^{-3} and a standard deviation one tenth as large as the mean. The resulting sample for the marginal distribution of f(x) at any x is shown in Figure 1. A gaussian PDF is overlaid, showing that modeling $f(\cdot)$ with a gaussian random field is quite reasonable in this case. The mean and standard deviation of f (x) are chosen to be 0.0316 and $0.396*10^{-3}$. The Ornstein-Uhlenbeck correlation function, given in (22), is used to describe the spatial structure of $f(\cdot)$. The value τ = 0:513 _ 10_3 is chosen, which gives a correlation of 0.95 at a separation of 100m and 0.60 at 1000m.

The PDF for the valve coefficient is chosen to be Gamma, with mean 49 and standard deviation 7. This choice for corresponds to the belief that most of the head loss in the pipeline is due to friction. Initially our beliefs about the leak location and size are taken to be very simple. The PDF for is chosen to be uniform on the interval (0,L), and the PDF for is chosen to be Gamma with mean 0.003 and standard deviation 0.003. This choice for corresponds to the belief that the leak will be small, of the order a few percent of total velocity. In section 6 we show how more careful modeling of the leak can be implemented.

Finally, for our beliefs about meter accuracy we choose independent gaussian PDFs for and , with mean zero and standard deviation equal to 1 percent of typical velocity.

4.2 RESULTS

The predictive distribution of is summarized using rejection sampling. Simple descriptions of the principles of this kind of sampling are given in Ripley (1987) and Smith and Gelfand (1992) while Robert and Casella (1999) provides further details, including extensions to the Markov chain Monte Carlo (MCMC) approach.

The simplest form of rejection sampling is used. First, a point is sampled from . Using this value and the data we can compute , as described in section 3, and then the likelihood value . The point is then kept or rejected with probability v/M, where

$$M = \sup_{\theta} \Pr(\epsilon = \bar{\epsilon} \mid \theta, \bar{Y}). \qquad (24)$$

For M we can use , which we know is at least as large as the supremum because has a gaussian distribution with zero mean. All the calculations were carried out in the R statistical programming environment.

The predictive distribution of is summarized in terms of High Density Regions (HDR). These are presented as isodensity contours bounding an area containing a designated amount of probability, in our case 95%, 50% and 20%. As these are computed from a finite sample they are estimates of the true HDR regions, and will show some sampling variation. Samples of size $4*10^4$ were used, as this seemed sufficient to give smooth sampled contours.

To generate some measurement data we set all uncertain values to their 70th percentile values: this is rather arbitrary but it avoids any suspicion that the results have been tuned in any way. The resulting leak descriptors are l = 700 and γ= 0.0361, and the measurements are

$$(\bar{r}_0^0, \bar{r}_L^0, \bar{r}_0^1, \bar{r}_L^1) = (1.63, 1.63, 1.66, 1.50). \qquad (25)$$

When analyzing the results the focus should not be on whether the probabilistic approach gets the prediction 'right' or not, as this depends in part on how consistent the measured data are with the engineer's prior knowledge: the choice of the 70th percentile is meant to be representative of 'moderate consistency'. What is more important is to get a feeling for the amount of uncertainty that remains in the predictive distribution, which is proxied by the area of the HDRs. It is this uncertainty that the deterministic mass imbalance approach leaves out.

The results for four different types of inference are shown in Figure 2. In the top left-hand panel we have the prior distribution of (l, γ). The iso-density contours from the true joint distribution are directly computable in this case, and they are shown using dashed lines, allowing us to get some feeling for the amount of variation induced by the finite sample. In the other three panels we have the three variations discussed in section 3.

Taking the standard case first, in the bottom left-hand panel, we see that a large amount of uncertainty remains after using the data $(\bar{r}_0^1, \bar{r}_L^1)$. Going by the 50% HDR, the leak location is restricted to the range (300, 1000), and the leak coefficient to the range (00002; 0.005). While this represents a large decrease on the prior ranges, it indicates that the kinds of uncertainties we have chosen, which do not seem extreme, have a very substantial impact on our ability to describe the leak. The key uncertainty in terms of its impact on our predictive variance is the meter error $\mathrm{Var}(\epsilon)$, for which it could be argued that our choice of a standard deviation of only 1% is rather conservative.

The upward slope of the iso-density contours in this panel indicates that the predictive distribution of (l, γ) is positively correlated. This is a consequence of the orifice equation (2a). A given amount of leakage arises as a trade-off between $h(\ell)$ and γ, where $h(\ell)$ is itself closely and positively related to $L - \ell$. If our data are not strong enough to pin down either ℓ or γ, then the result will be a range of predictive values in which increased values for ℓ may be offset by increased values for γ.

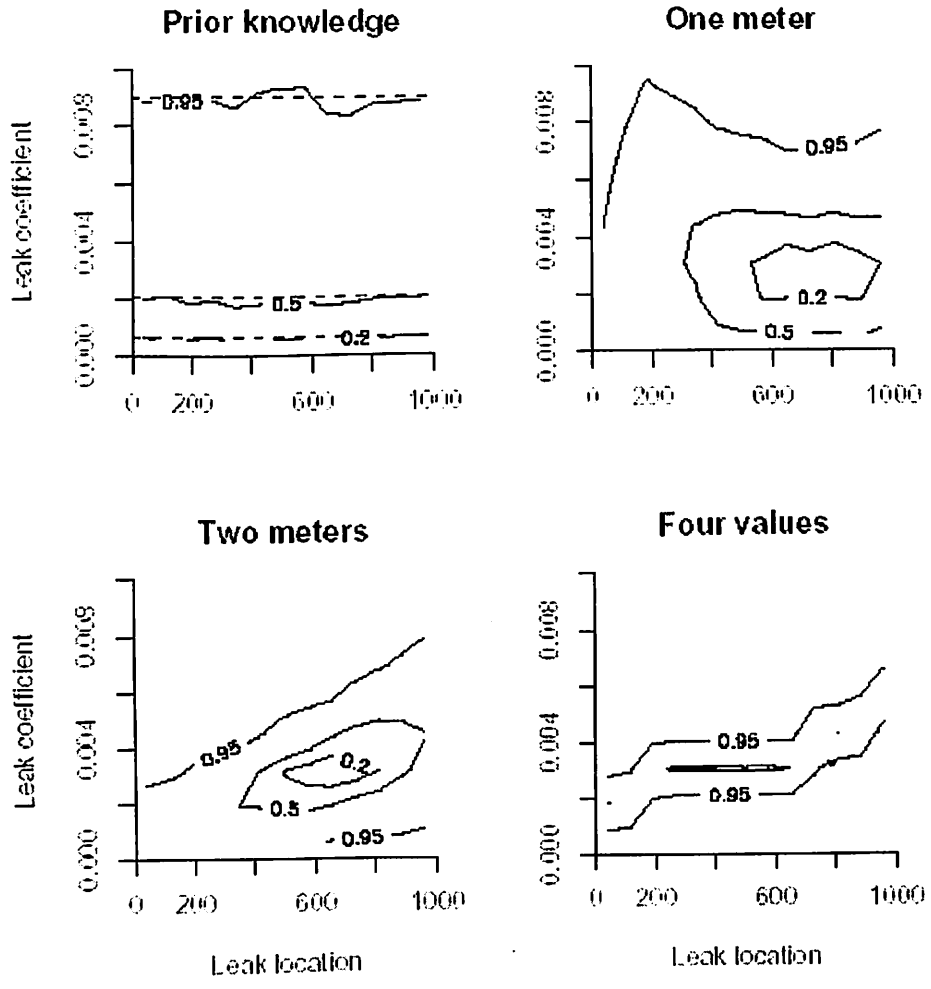

Figure 2: High density regions (95%, 50% and 20%) for the predictive distribution of leak location ℓ and leak coefficient γ for four different sets of measurements. The top lefthand panel is prior to the data (the true values are shown as dashed lines, to show the amount of variation induced by the finite sample). The data in the remaining panels are $(\bar{v}_0^1, \bar{v}_L^1)$ for 'Two meters'; $(\bar{v}_L^1)$ for 'One meter'; and $(\bar{v}_0^0, \bar{v}_L^0, \bar{v}_0^1, \bar{v}_L^1)$ for 'Four values'.

In the top right-hand panel we have the one-meter case, in which the datum is the single observation $\bar{v}_L^1$. This is the case for which the mass imbalance method cannot give an answer. Contrasting this panel to the two-meter case, we can see that the uncertainty, e.g. as measured by the extent of the 50% HDR, is much larger, although still much less than the prior, particularly with regard to leak location.

In the bottom right-hand panel we have the two meter case with pre- and post leak observations, i.e. the dataset $(r_0^0 \quad r_L^0, r_0^1, r_L^1)$. As mentioned in section 3.3 this is effectively a `free upgrade' to the standard case in the bottom left-hand panel. What is surprising is how much difference it makes: the 90% HDR is perhaps one-fifth the size of that in the standard case. The reason is that, as mentioned above, the meter error is a key factor in determining the predictive variance. The extra observation allows us to incorporate information directly relevant to that error, since $r_0^0 \quad r_L^0 = \eta_0 - \eta_L$. With the effect of meter error reduced, the positive correlation between ` and that arises from the orifice equation is even more clearly visible.

5 LEAK DETECTION AND ATTRIBUTION

In the previous section the engineer's knowledge about the leak was modeled very crudely. In this section we show how more complicated knowledge can be represented, within a more general framework in which we classify the leak according to a type. In this case the probabilistic approach encompasses leak attribution as well as leak description, i.e. we can compute the probability that the leak is of each of the specified types. If we include among our types a `no leak', then attribution extends to leak detection, i.e. we can compute the probability that a leak has occurred.

We define a classifying variable $T \in \{0, 1, \ldots, T\}$, which denotes whether the pipeline has a leak, and what type of leak it is. Let $T = 0$ denote no leak. All of our calculations so far have been predicated on the notion that there has been a leak, even if only a very small one, i.e. they have been conditioned on $T > 0$. Let $T = 1$ denote the leak described in section 5, which we will call an `Ordinary Leak'. For the ordinary leak we have

$$\Pr(\ell, \gamma \mid \text{ordinary}) \propto 1(\ell \in (0, L)) \times \text{Gamma}(\gamma; a = 1, s = 0.003) \qquad (26)$$

Where 1(P) is the indicator function of the proposition P. The first term is for the uniform distribution on (0,L), while the second is the gamma PDF with shape parameter a and scale parameter s, which satisfies

$$\text{Gamma}(\gamma; a, s) \propto \gamma^{a-1} e^{-\gamma/s}. \qquad (27)$$

The mean and variance of a Gamma random variable are as and as2, respectively. For ordinary leaks the values a = 1 and s = 0.003 correspond to both the mean and the standard deviation being 0.003 (the speçial case with a = 1 is known as an exponential distribution). Note that users of computer software that can generate Gamma random variables should be alert to the fact that the two parameters can be specified in different ways; the version given in (27) corresponds to the R statistical programming environment.

Now we introduce a second type of leak. Suppose that the engineer was worried about sabotage along a section of the pipeline that ran alongside an access road. For leaks of this type we must have l restricted to the section accessible by road, and the leak size might be much larger: say 5 times as large. Therefore the Sabotage Leak has

$$\Pr(l, \gamma \mid \text{sabotage}) \propto 1(l \in S) \cdot \text{Gamma}(\gamma; a = 1, s = 0.015) \qquad (28)$$

Where $S = (0, L)$ is the accessible section of the pipeline. The choices a = 1 and s = 0.015 in (28) follow from our previous choice, where the scale parameter is 5 times larger than in the ordinary leak case. For the accessible section we choose S = (300, 800) for our example. We complete this more general model by assigning a probability to each of the types. In section 5 we have $T = 1$ with probability 1, so that $\Pr(T = 0) = 0$. Now if the engineer believed that the pipeline was very leak-prone then setting $\Pr(T = 0)$ close to zero might indeed be appropriate. But if the pipeline was thought to be tight, then we would be more inclined to treat data suggesting a small difference between v_0 and v_L as indicative of measurement error. In other words, for a tight pipeline $T = 0$ would have a probability close to 1. For our example we suppose that the pipeline is quite leak-prone, and set

$$\Pr(T = i) = \begin{cases} 0.5 & i = 0 \text{ (no leak)} \\ 0.4 & i = 1 \text{ (ordinary leak)} \\ 0.1 & i = 2 \text{ (sabotage leak)} \end{cases} \qquad (29)$$

Although as we have restricted our modeling to three leak-types, we should rename the 'ordinary' leak to the catchall 'other unspecified leak'. For the inference we can incorporate T among the uncertain parameters θ. Then when we compute the predictive distribution of θ and we are also computing the probability distribution of T conditional on the velocity data. In other words, we can use the probabilistic approach to turn the data into an assessment of whether there has been a leak, and on the condition that there has been a leak -what kind of leak it is.

We illustrate this with the example from section 5. In that example we had . We reconsider this leak within the more general framework, and also consider two other leak coefficients, one twice as large, and one four times as large. These three scenarios are denoted as A, B (2*) and C (4*). The velocity data from the three scenarios are

Scenario A	1.66	1.59
Scenario B	1.69	1.55
Scenario C	1.73	1.47

(30)

Figure 3 shows the detection and attribution probabilities for each of the three scenarios, in the top left-hand panel, along with the HDR for leak location and leak coefficient in each case. The probabilities show that in scenario A there remains a small probability that , i.e. that no leak has occurred, and that the difference between measured upstream and downstream velocities is attributable to meter bias. In the second and third scenarios, for which the difference between the upstream and downstream velocity measurements is larger, the probability that is effectively zero. The other three panels show that as the leak type

probability shifts from so the predictive distribution of the leak location and coefficient also shifts. In scenario C the probability strongly favors a sabotage leak, and we see that most of the leak location probability is contained in the sabotage leak section of the pipeline. The more those different types of leak have different `signatures' in location and size, the more sensitive and effective will be the leak attribution. The approach outlined in this section can easily be extended to consider multiple leaks arising from the same or different causes.

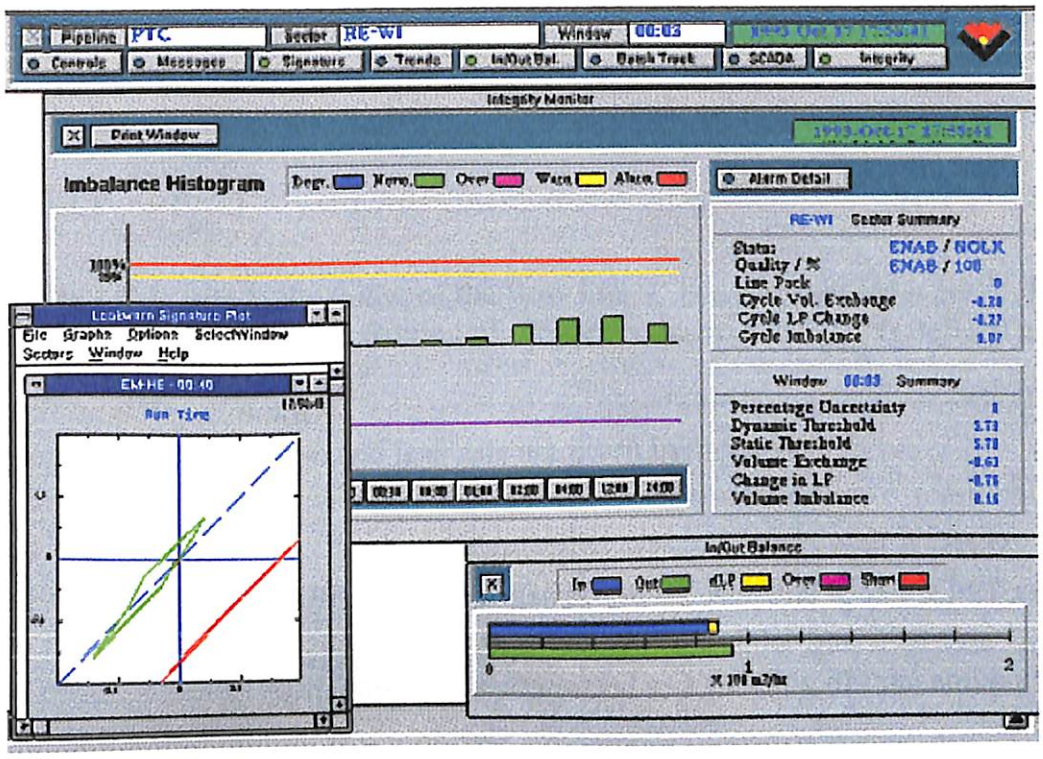

Source: Simulations Inc.

Fig. 2.2.2: Leak Detection by Real Time Transient Modeling

C.

1. ANALYTICAL MODELING

The single-phase leak equation for gas flow in terms of inlet and outlet pressure is given by:

$$q = C F_L (P_{in}^2 - P_{out}^2)^n \quad \text{.....(6.1)}$$

Where q is the gas flow rate at the outlet of the flow line, C is a constant for a particular pipe, n is normally 0.5 and F_L is the reduction of efficiency due to a leak. F_L is defined as:

$$F_L = [1 + L_{LD}(q_{LD}^2 + 2 q_{LD})]^{-n} \quad \text{.....(6.2)}$$

and the dimensionless leak location and leak rate are given by:

$$L_{LD} = L_L / L_P \quad \text{.....(6.3)}$$

$$q_{LD} = q_L / q \quad \text{.....(6.4)}$$

Where L_p is the length of the pipeline, L_L is the distance to the leak and q_L is the leak rate from the pipeline. As shown by Scott, S.L et al (1999), the outlet gas flow rate in a multiphase flow line experiencing a leak can be expressed as a function of inlet and outlet pressure in the following form

$$q_{sc} = F_{leak} (F_{2\text{-}\varphi})_q (C Z T f_{SG} L_p / d^5)^{-0.5} (P_{in}^2 - P_{out}^2)^{0.5} \quad \text{.....(6.5)}$$

where C is a constant, Z is the real gas compressibility factor, d is the diameter of the pipe and f is the friction factor. The subscript "SG" denotes superficial single-phase conditions. The additional term ($F_{2\text{-}\varphi}$), which is called the two-phase (2-φ) efficiency is defined as

$$F_{2\text{-}\varphi} = (dP/dx)_{SG} / (dP/dx)_{2\text{-}\varphi} \quad \text{.....(6.6)}$$

Comparing equations 6.1 and 6.5, the additional two-phase term creates a flow regime dependent term, which separates the single-phase flow leak from the multiphase flow leak. This two-phase term creates a change in the response making it much more difficult to detect a leak in a multiphase flow line. However, this type of analysis makes it possible to examine the performance of momentum (friction) loss leak detection methods to determine what size and location of leaks can be detected. This provides greater confidence and understanding than the "black box" approach taken by most leak detection suppliers. As shown by Scott et al. (1999), these methods provide for rapid detection of leaks but have been shown to be high depended upon the location of the leak. This attribute does not fit well with arbitrary detection limits but can act to reduce detection time and will function even without a measurement of flow rate at the inlet of the pipe.

For flow lines where inlet metering is not practical, such as sub sea, special testing requirements may be needed to optimize these data driven momentum balance methods. In particular, periodic testing such as the deliverability testing of gas wells, would provide an accurate and up to date estimate of the $F_{2\text{-}\varphi}$ term.

2. SIMULTANEOUS SHUT-IN TEST (SSIT)

To emphasize the difference in single and multiphase flow on leak detection a Simultaneous Shut-in Test has been performed using the transient simulator OLGA. Table 6.1 shows the basic data used for the simulation runs detailed in this chapter. An example OLGA input file is given in Appendix-A. As can be seen three different leak locations were investigated

Table 6.1
Typical Data for Simulation

Parameter	Value
Flowline Size (inches)	8" NB
Flowline Length (m)	4,360 m
Leak Location (Distance from wellhead, m)	Near (875 m) Middle (2,600 m) Far (4,270 m)
Leak Size (inches)	1" – 4"
Backpressure for leak (psia)	15

The first case examined is the shut-in response for a pipeline experiencing a leak. The first step is to shut in the pipeline at both the ends i.e. at the wellhead (done remotely from the platform) and at the separator. The response for single-phase gas and for multiphase (volatile oil) is presented here. For a gas pipeline no leak case the pressure stabilized to an average value with time. In the presence of a leak a drastic pressure drop can be observed at both ends, even for a small leak.

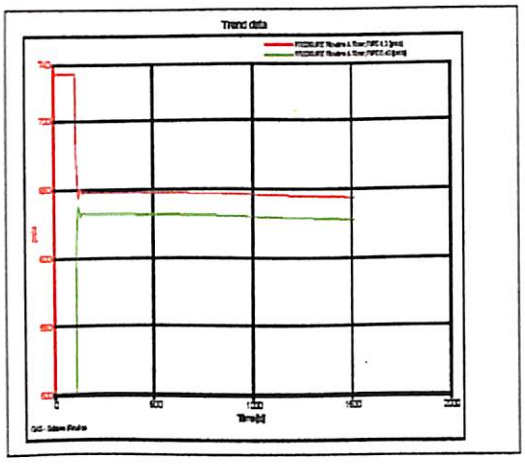

Fig 6.1 (a) Pressure Transient for Pipeline Without Leak

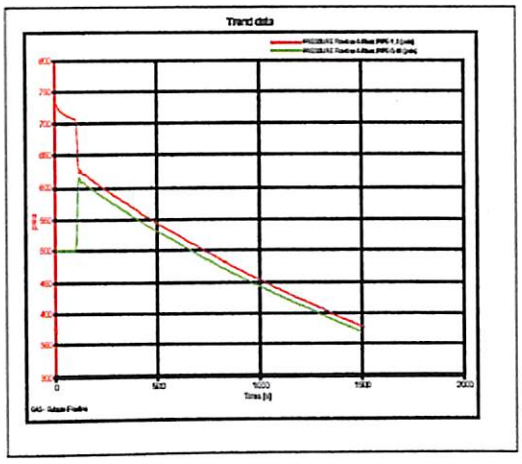

Fig 6.1 (b) Pressure Transient for Pipeline with a Leak

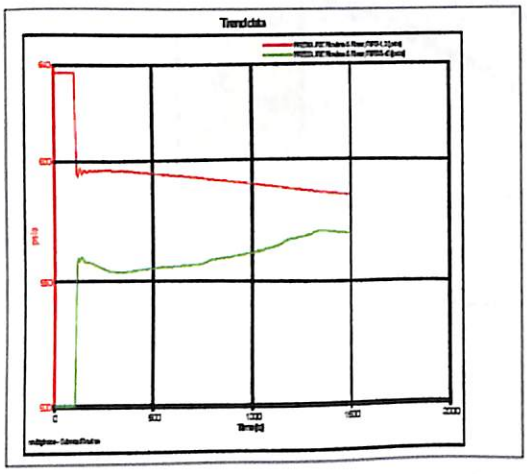

6.2(a) Pressure Transient for Pipeline without a Leak (Multiphase)

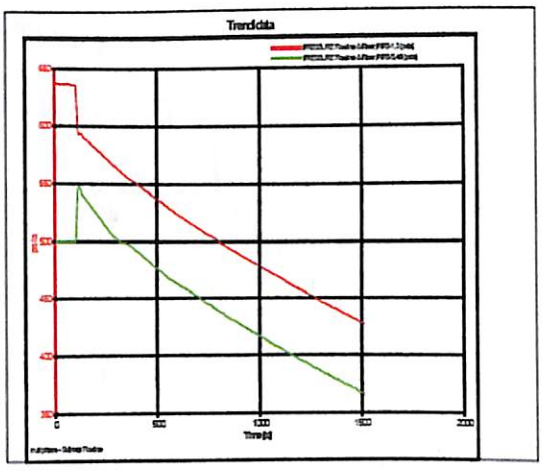

6.2(b) Pressure Transient for Pipeline with a Leak (Multiphase)

For a multiphase pipeline the pressure does not stabilize even for the no-leak case. It is very difficult to determine whether the pressure variation is because of multiphase flow or because of the leak.

Effect of Flow Regime on Detection of Leak

The discontinuities in superficial gas and liquid velocities created at the leak point show very obvious indication of a leak. These changes in superficial gas velocity in gas and liquid also change the liquid holdup and this in turn creates a heavy change in pressure drop.

The multiphase flow can be categorized in the following flow regimes

Distributed flow

- Bubble flow
- Slug flow

Separated flow
- Annular flow regime
- Stratified flow regime

Bubble flow

The Pressure profile for different leak sizes is shown in figure 6.3(a). The leak location is the middle of the flow line for the following plots. The pressure profile changes considerably when there is a change in the flow regime i.e. for extremely high leaks.

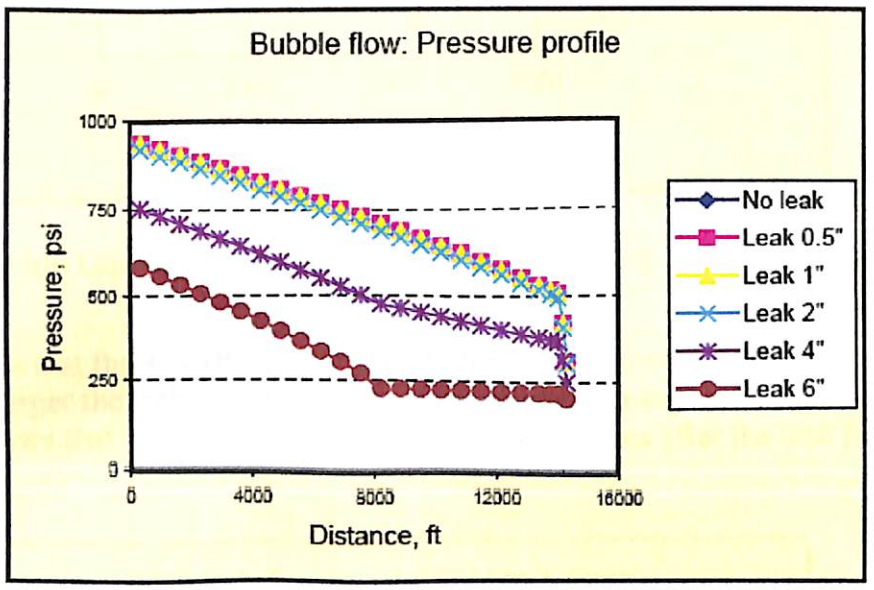

Fig 6.3(a): Pressure Profile for Increasing Leak Size

Figure 6.3(b) shows that the liquid holdup decreases with increase in leak size, where "10" denotes a 1-inch leak size, "20" denotes a 2-inch leak size, etc. For very large size the change in liquid holdup is pronounced. The liquid holdup decreases more before the leak point than after the leak point.

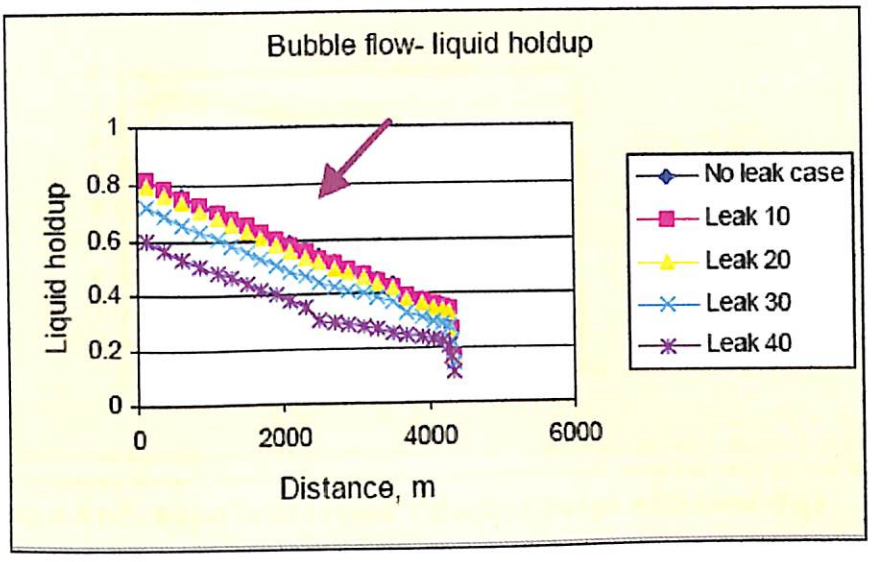

Fig 6.3(b) Liquid Hold Up in Bubble Flow with Increasing Leak Size

Fig. 6.3 (c) shows that the superficial gas velocity for bubble flow increases before the leak point. The larger the leak size the greater is the increase in superficial gas velocity. Figure 6.3(d) shows that the superficial liquid velocity decreases after the leak point.

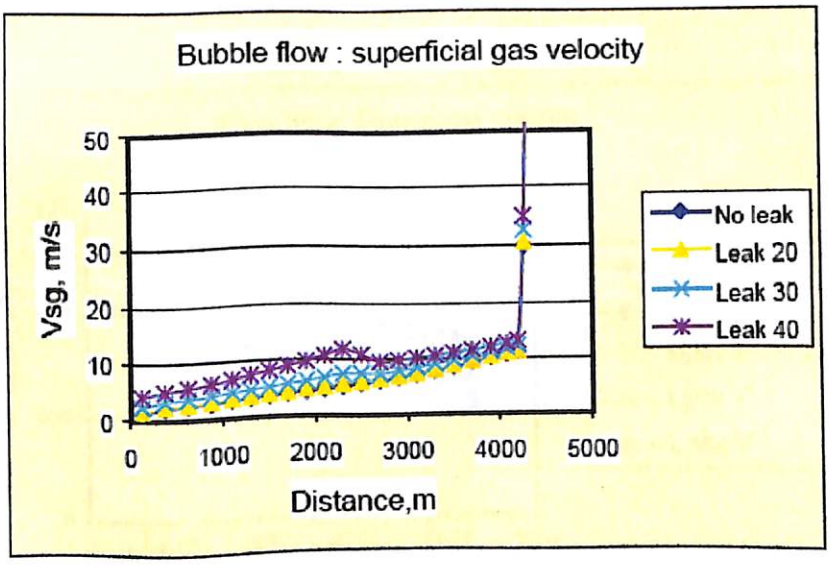

Fig 6.3 (c): Superficial Gas Velocity with Leak Size

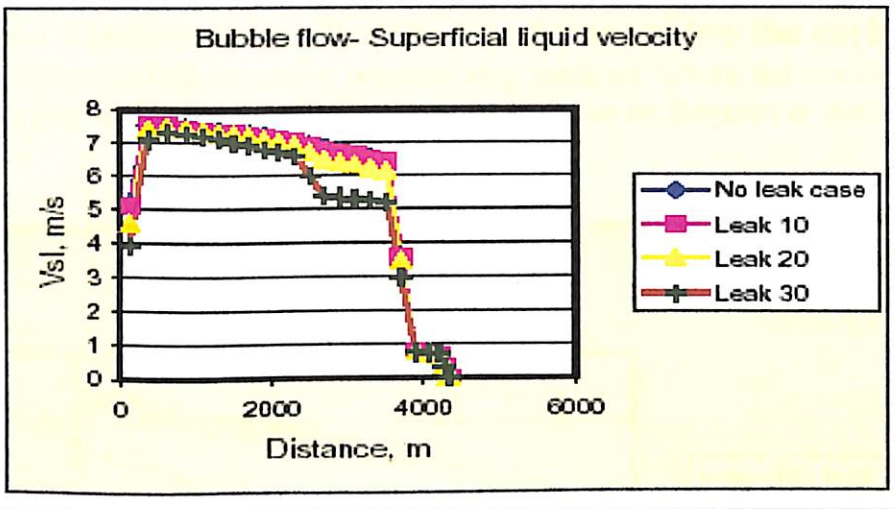

Fig 6.3 (d): Superficial Liquid Velocity Change with Leak Size

The flow regime downstream of the leak changes from bubble to stratified flow. The decrease in superficial liquid velocity downstream of the leak changes the flow from bubble flow (distributed) to stratified flow (separated). The bubble flow behaves more like a single-phase liquid. It is very easy to detect leaks in bubble flow.

Slug flow

Fig 6.4(a) shows that the pressure profile changes due to a leak in a flowline operating in slug flow are only significant when the flow regime changes as a result of the leak.

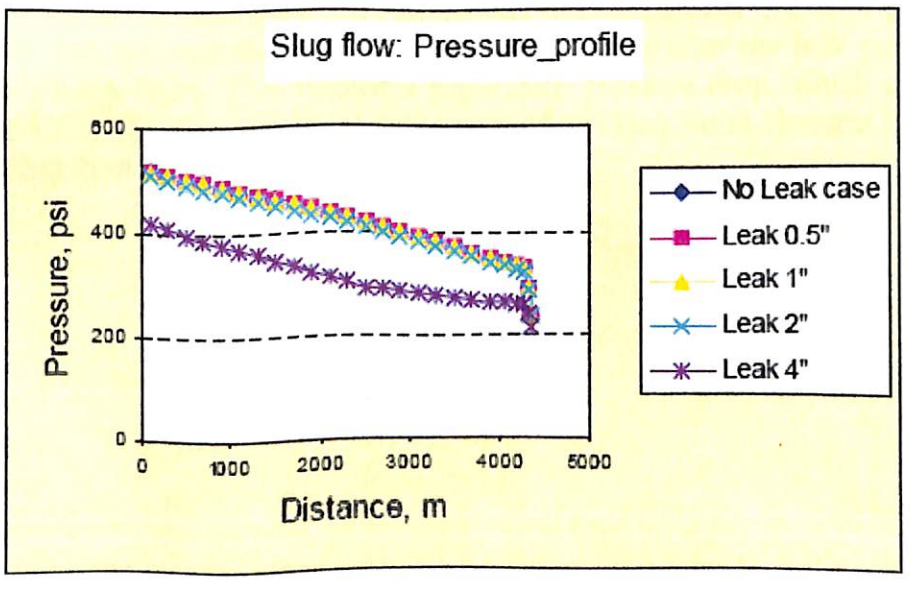

Fig 6.4(a): Pressure Profile with Varying Leak Size

Figure 6.4(b) shows that the holdup decreases only for very large leaks. Unless the liquid holdup decreases drastically, there will not be enough pressure drop that can be detected by PSL. More effective leak detection requires slug tracking, where the number of slugs and slug length play an important role in whether a leak can be detected or not.

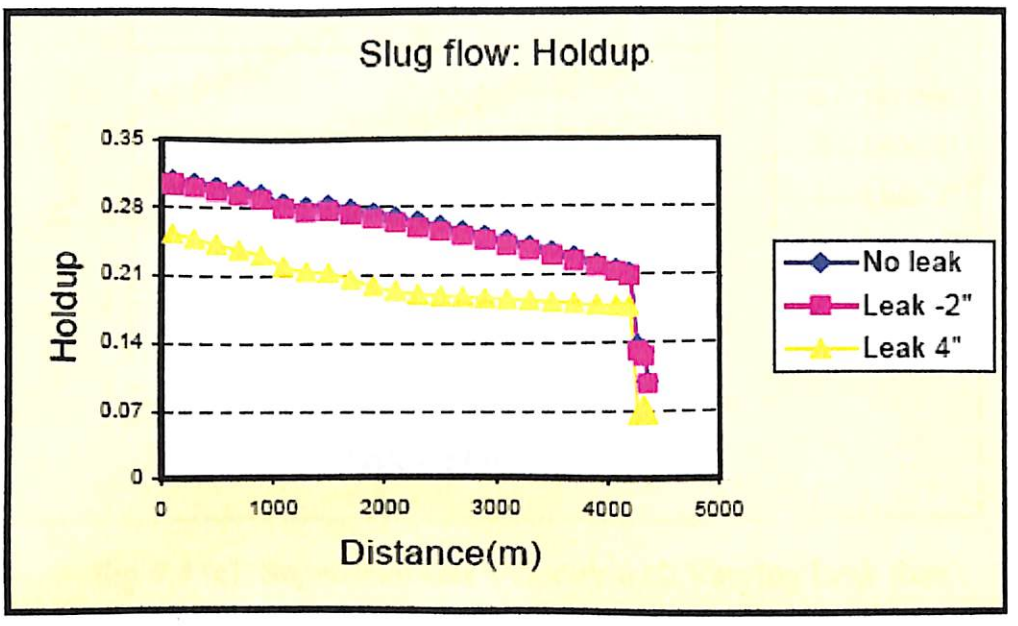

Fig 6.4(b): Holdup for Various Leak Sizes

Figure 6.4 (c) shows that the superficial gas velocity changes only for large leaks, it increases significantly before the leak point and decreases after the leak point. Figure 6.4(d) shows that the superficial liquid velocity decreases after the leak point, however only for very large leaks. This creates a significant pressure drop, which can easily be detected by PSL. The flow regime downstream of the leak point changes after the leak point from slug flow to stratified flow.

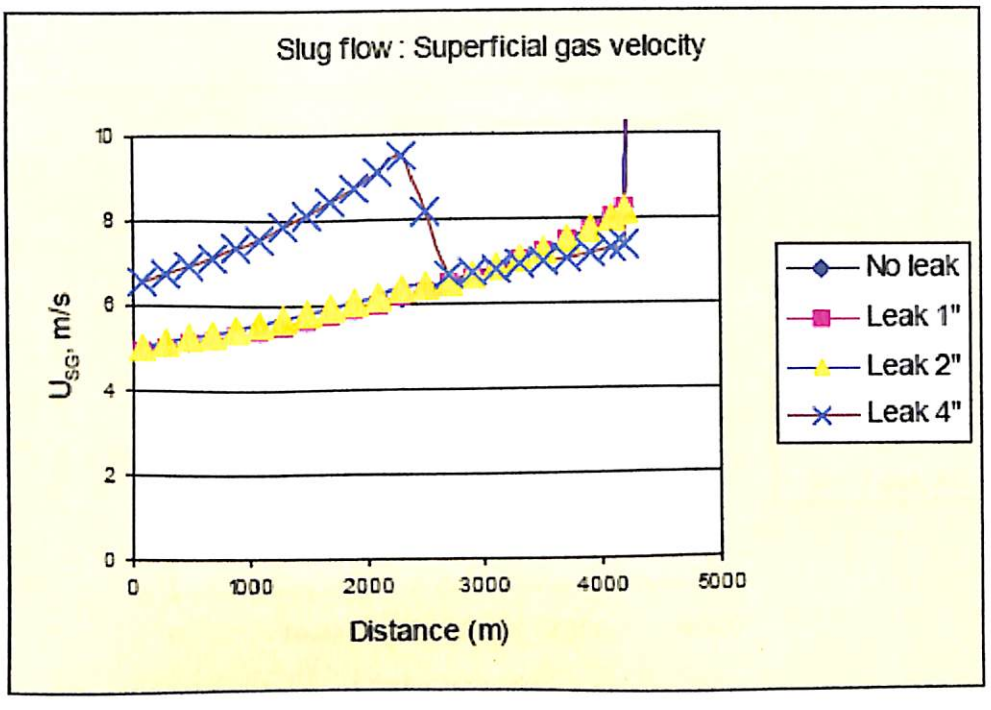

Fig 6.4 (c): Superficial Gas Velocity with Varying Leak Size

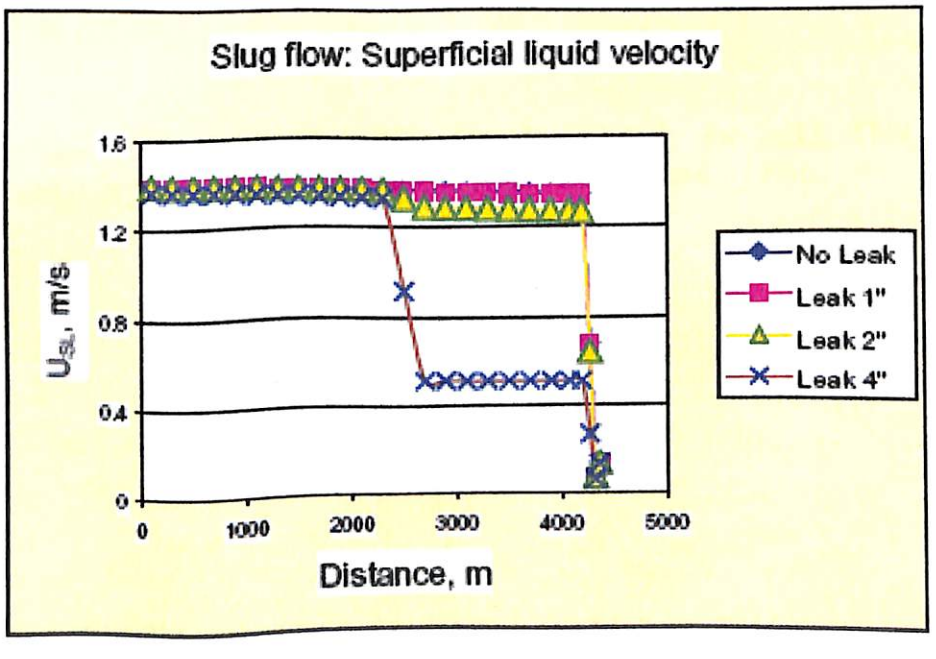

Fig 6.4(d) Superficial Liquid Velocity with Varying Leak Size

Annular flow

Fig 6.5(a) shows that the pressure profile for annular flow changes significantly with varying size of leaks.

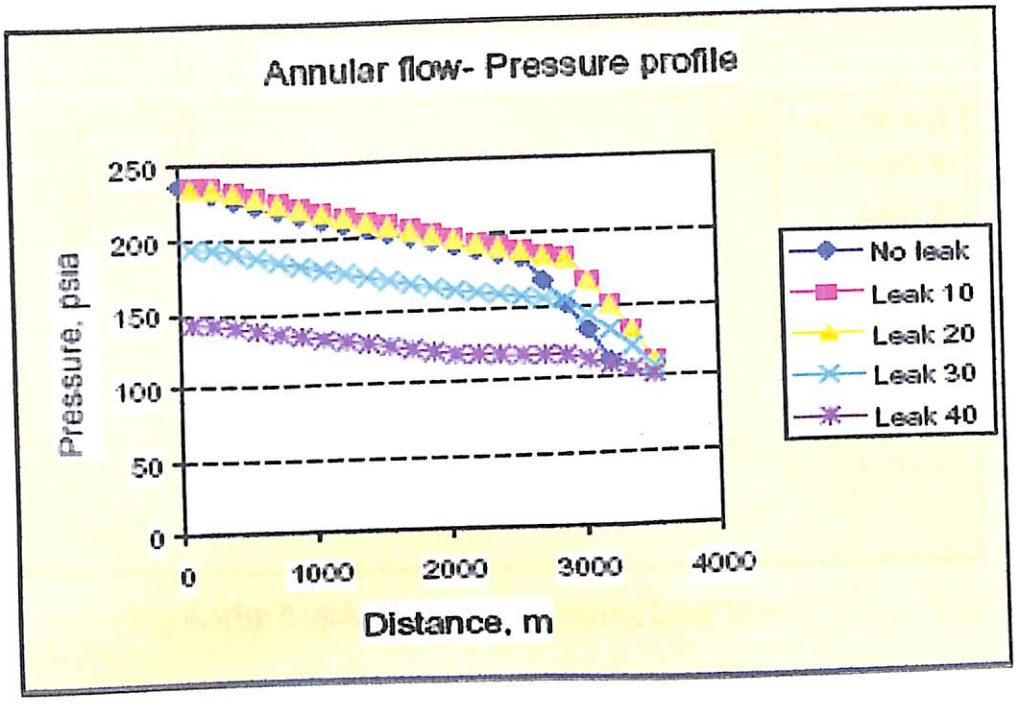

Fig 6.5(a): Pressure Profile with Varying Leak Size

Figure 6.5(b) shows that the holdup decreases dramatically for leaks. This creates a significant change in pressure drop, which can easily be detected by PSL.

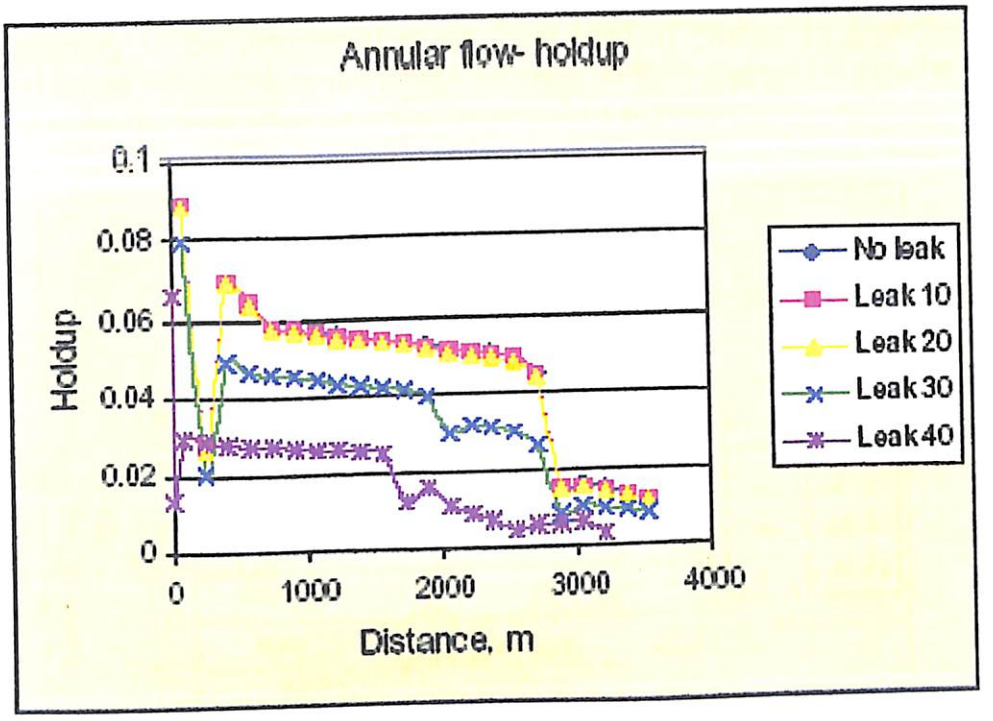

Fig 6.5(b): Liquid Holdup for Varying Leak Size

Figure 6.5 (c) shows that the superficial gas velocity (v_{SG}) does not change much for small leaks and there is a small increase in v_{SG} for large leaks.

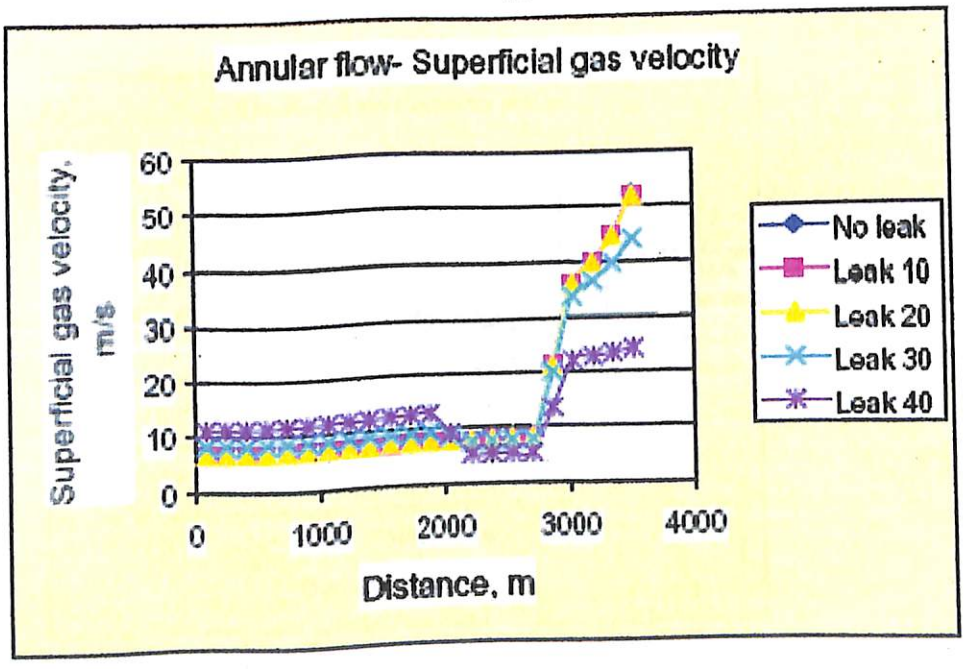

Fig 6.5(c): Superficial Gas Velocity Profile with Varying Leak Size

Figure 6.5(d) shows that the superficial liquid velocity increases before the leak point. This is contrary to the distributed phase. This kind of change in superficial gas and superficial liquid velocity does not create a change in flow regime for annular flow. Even after large leaks the flow remains in the annular flow regime.

z

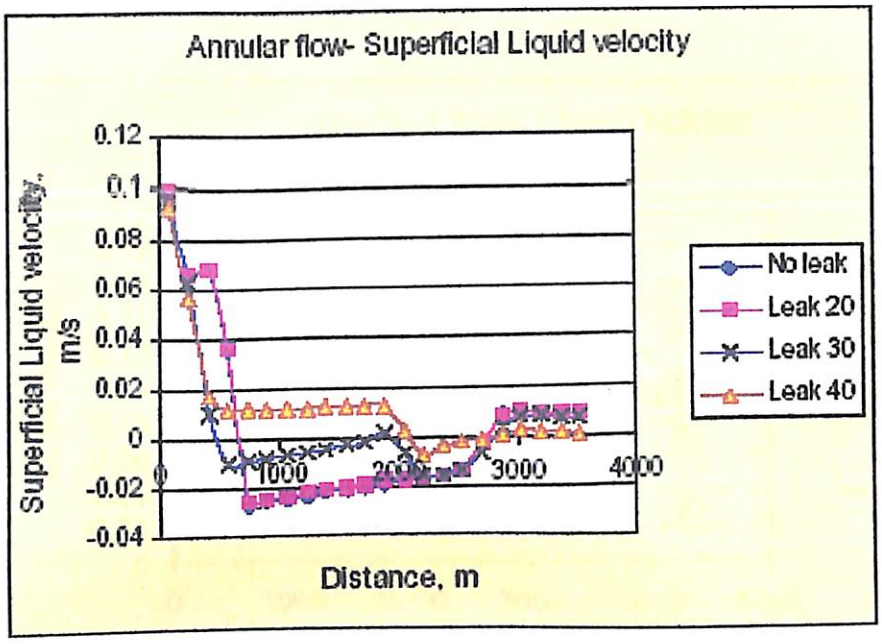

Fig 6.5(d): Superficial Liquid Velocity Profile with Varying Leak Size

Stratified flow

Fig 6.6(a) shows that the pressure profile for stratified flow changes significantly only for large leaks.

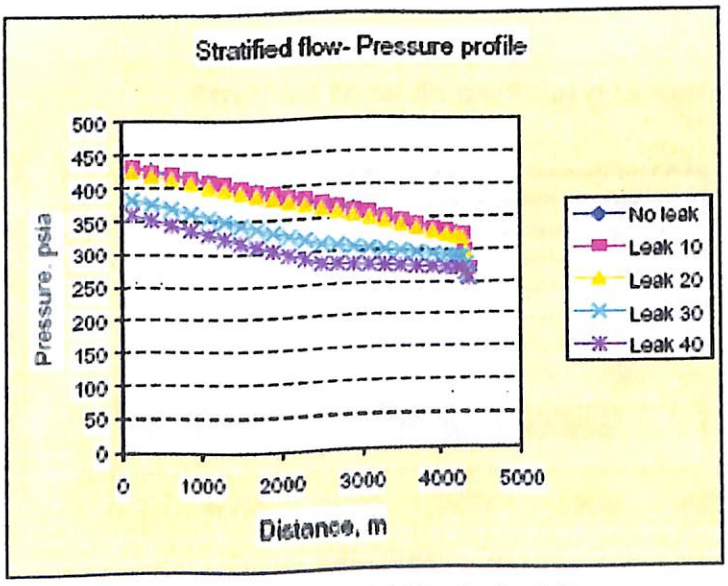

Fig 6.6(a): Pressure Profile with Varying Leak Size

Figure 6.6(b) shows that the holdup decreases for leaks. This creates a change in pressure drop, which can be detected by PSL. For stratified flow the only way to detect a leak is dependent on liquid holdup. A more elaborate analysis with Lockhart Martinelli parameter will help to understand when leaks in stratified flow can be detected.

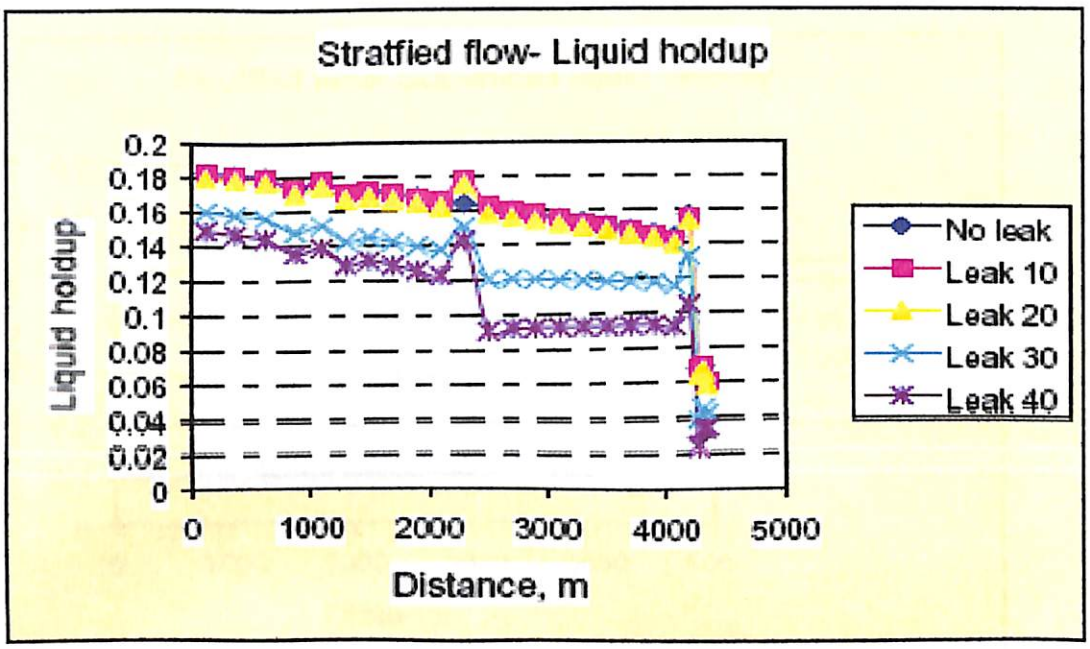

Fig 6.6(b): Liquid Holdup for Varying Leak Size

Figure 6.6 (c) shows that the superficial gas velocity increases before the leak point.

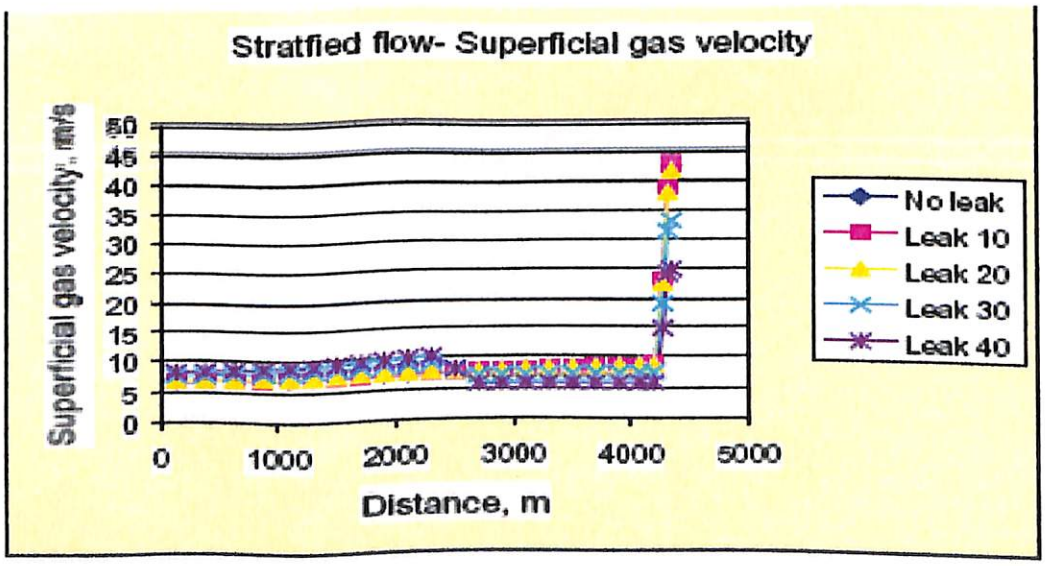

Fig 6.6(c): Superficial Gas Velocity for Varying Leak Size

Figure 6.6(d) shows that the superficial liquid velocity decreases after the leak point. This kind of change in superficial gas and superficial liquid velocity does not create a change in flow regime for Stratified flow. Hence even after large leaks, the flow will remain in the stratified flow regime.

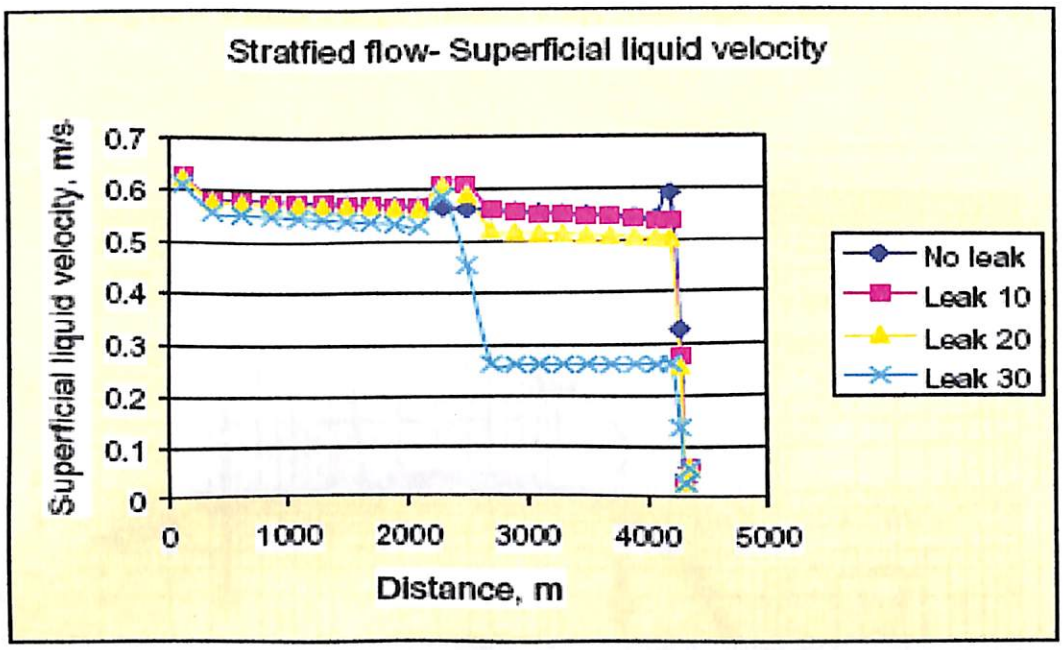

Fig 6.6(d): Superficial Liquid Velocity with Varying Leak Size

Change in Flow Regime Due To Severe Leak

Figure 6.7 shows that for very large leaks with distributed flow (bubble flow, slug flow) there is a change in flow regime downstream of the leak. The drop in superficial liquid velocity (v_{SL}) downstream of the leak is so large that the flow becomes stratified flow. For the case of separated flow (stratified flow, annular flow) the change in v_{SL} cannot create any change in the flow regime. This change in flow regime for the case of bubble flow and slug flow creates a large pressure drop, which can be easily detected by PSL's.

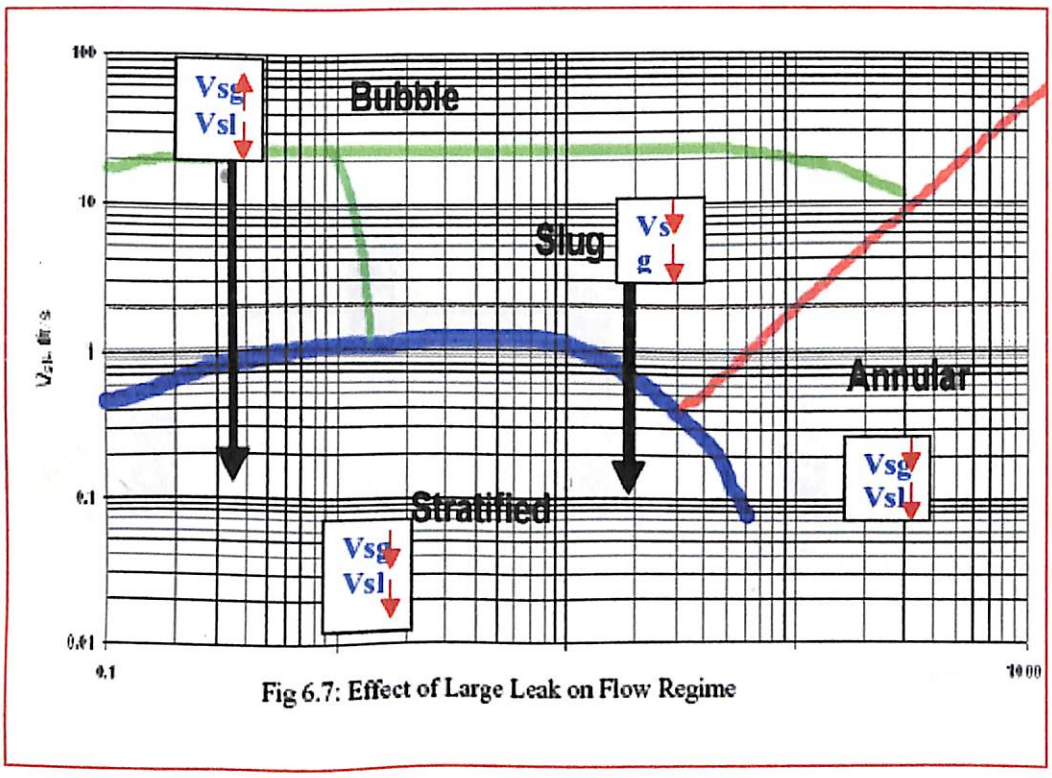

Fig 6.7: Effect of Large Leak on Flow Regime

Response Time for Detection of Leak

Figure 6.8 shows the response time for same size of leak to stabilize in the various flow regimes. The response is best for annular flow and worst for slug flow. It is in line with the observation that the response time for detection of leak in gas lines is better than in oil lines.

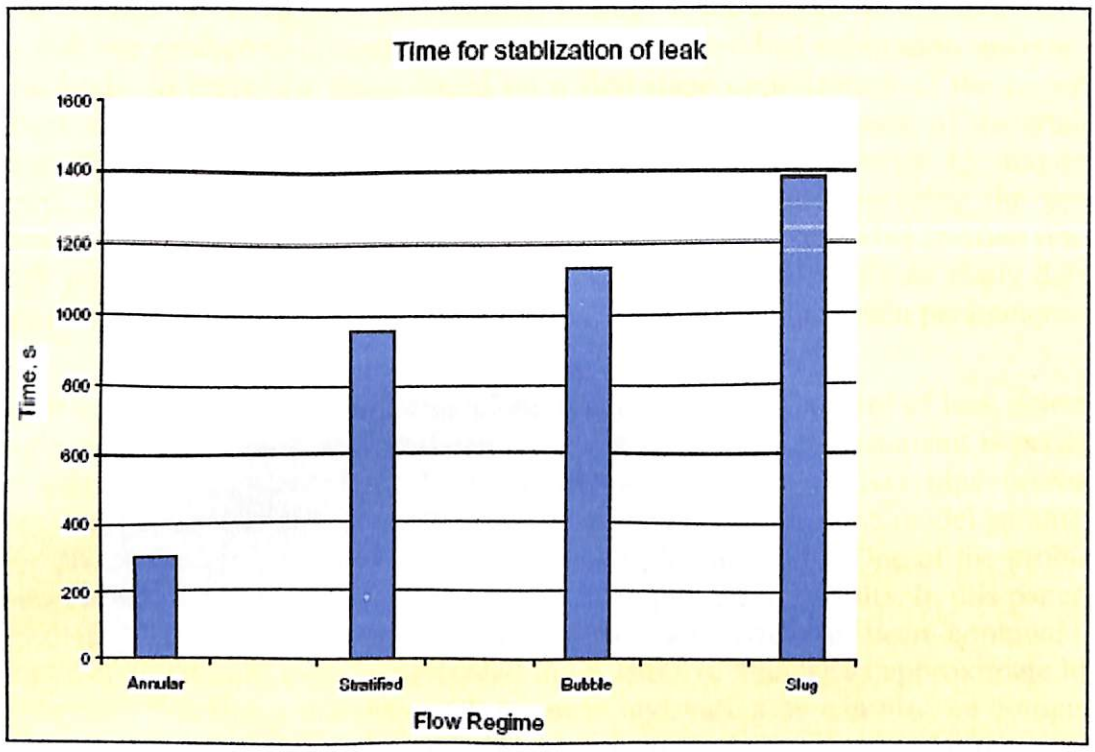

Fig 6.8: Transient Response-time for Stabilization in Various Flow Regimes

The response time for detection of leak in separated flow (Annular flow, Stratified flow) is better than that for distributed flow (Bubble flow, Slug flow).

D. CONCLUSION

The activity of leak detection in the presence of uncertainty is an example of a statistical 'calibrated prediction'. That is, we want to predict certain quantities such as the leak location and leak size, but we need at the same time to calibrate our model to imperfect data in order to reduce our uncertainty about quantities such as the pipe roughness and the valve settings. Within a fully probabilistic setting we are able to do this in a way that ensures that our predictive uncertainty accounts for our residual calibration uncertainty. Other methods, in particular those based on a first-stage optimization of the uncertain parameters in the model, are not able to provide an adequate measure of uncertainty. Insofar as the optimization approach can be considered to be inference by maximum likelihood, the basic condition that justifies an uncertainty analysis using the profile likelihood is that there is a reasonable amount of independent data. This is often not the case with pipelines and pipe networks, where there are typically only as many data as there are meters, and often there are fewer meters than there are uncertain parameters.

This paper has outlined the fully probabilistic treatment of the problem of leak detection in a single pipe, using the mass-imbalance approach. However, the treatment is perfectly general, and may be extended straightforwardly to models that cover pipe networks, providing that each evaluation of the model at a particular choice of the model parameters is quick. This is certainly the case for simulators of pipe networks. One of the problems that can arise with a probabilistic treatment is how to present the results. In this paper the predictive distribution describing the leak location and size has been computed by sampling. The results can then be presented in an intuitive manner as approximate high-density regions. Summary statistics such as mean and variances can also be computed, but the graphical presentation is probably easier to interpret if a rapid response is required. The paper also shows how we may generalize the problem of leak description, premised on a single 'typical' leak, to leak detection and leak attribution based on a number of scenarios describing possible events, and the types of leak that might follow. In this case the probabilistic approach allows us to assign a probability to each scenario and to update that probability using data from meters. A probabilistic description of our uncertainty about the pipeline feeds naturally into a decision-theoretic framework for establishing the most effective response. . For example, the measured value of the upstream velocity after the leak has occurred is $\bar{v}_0^1$.

.

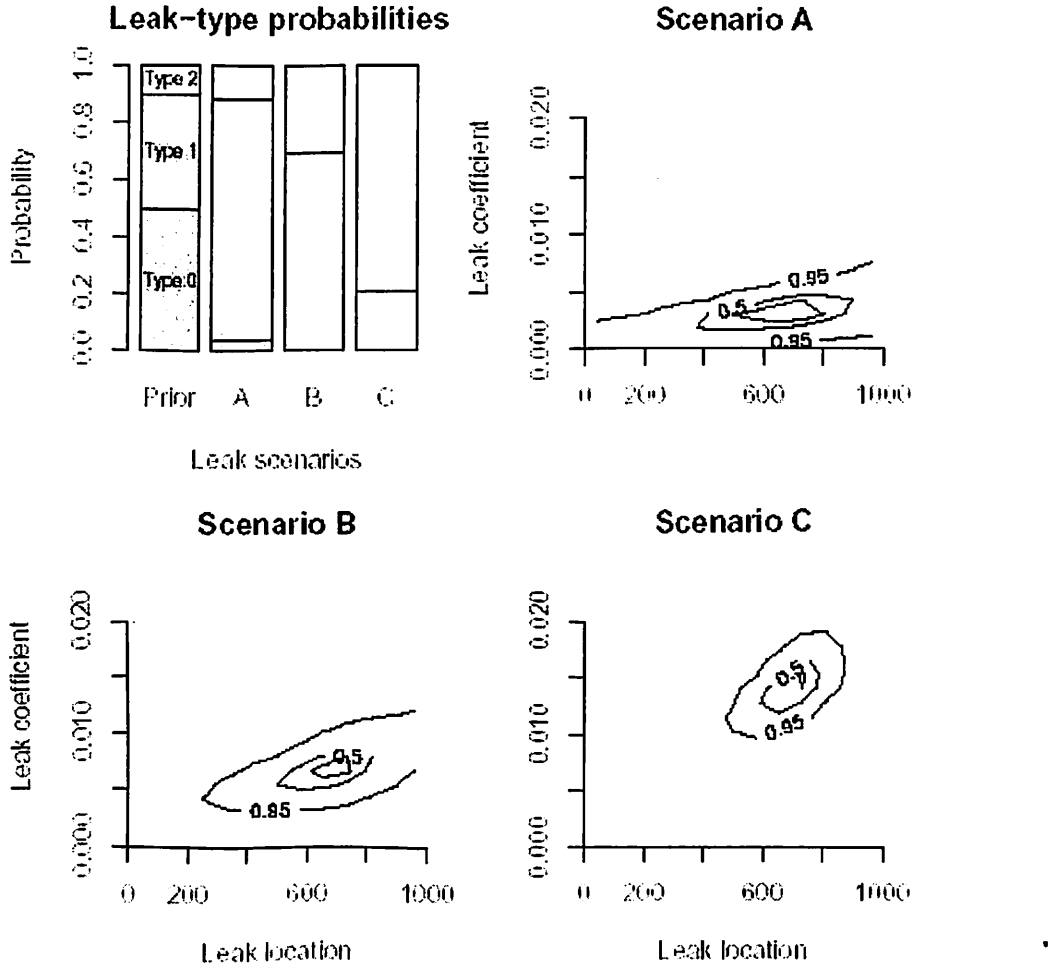

Figure 3: Leak detection and classification. The top lefthand panel shows the prior and predictive probabilities on the three types of leak (0: no leak; 1: ordinary leak; 2: sabotage leak). The three scenarios correspond to three different sets of velocity measurements, given in (30). The remaining panels show the high density regions for the predictive distribution of leak location and coefficient in the 'Two Meter' case, conditional on a leak having taken place, for each of the three scenarios.

Notation

Quantities and functions

D = Pipe diameter (assumed constant)
ϵ_0, ϵ_L = Velocity meter measurement errors (collectively ϵ)
$f(\cdot)$ = Weisbach friction factor along the pipeline
g = Gravitational acceleration
γ = Leak coefficient
H, $h(\cdot)$ = Piezometric head at the upstream end of the pipeline, piezometric head along the pipeline
$K(\ )$ = Equivalent sand-roughness along the pipeline
k = Downstream valve coefficient
L = Pipeline length
$\rho(\ )$ = Definite integral of $f(\ )$, see eq. (11b)
Re = Reynolds number
S = Region of the pipeline in which a sabotage leak might occur
T = Leak type indicator
θ = Collection of parameter values
v = Fluid velocity without a leak
v, v_0, v_L = Fluid velocity, upstream and downstream fluid velocity (collectively V); a superscript 0 denotes prior to the leak, and 1 denotes post-leak
x, z, d = Index variables for distance along pipeline

Random field for the Weisbach friction factor

$\mu_1(\cdot)$, $\mu_2(\cdot,\cdot)$ = Mean function and covariance function of $f(\cdot)$
σ^2 = Variance of the stationary random field for $f(\cdot)$
$r(\ )$ = Correlation function of the stationary random field for $f(\cdot)$
τ = Decay rate of the Ornstein-Uhlenbeck stationary random field for $f(\cdot)$

Probabilistic operators and related quantities

$\mathrm{P_I}(\ )$ = Probability density function
$\mathrm{E}(\ )$, $\mathrm{Cov}(\ ,\ )$ = Expectation and covariance
a, s = Shape and scale parameters for the gamma distribution
c = Constant of proportionality
'$\cdot$' = 'Conditional upon', in probability distribution functions and covariances

Other symbols

'$\triangleq$', '$\equiv$' = 'Defined as', 'Equivalent by definition'

Measured values of previously uncertain quantities are denoted with an over-

E. GRAPHICAL INTERPRETATION

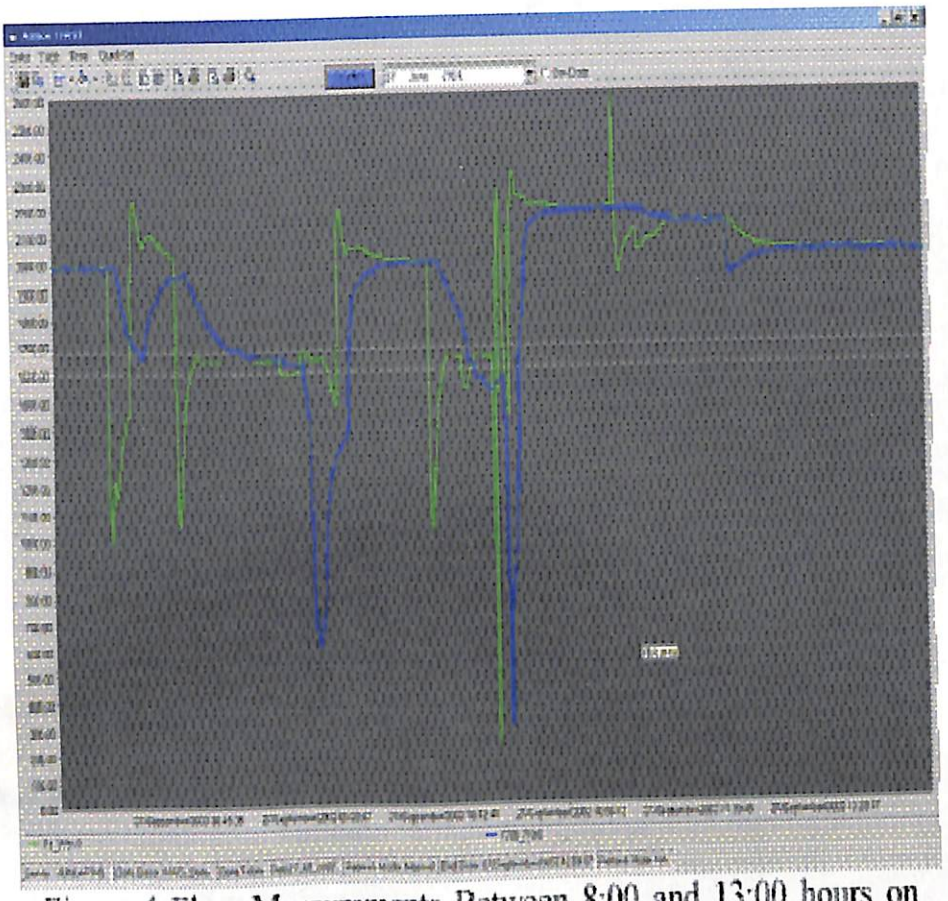

Figure 4 Flow Measurements Between 8:00 and 13:00 hours on 27/September/2002

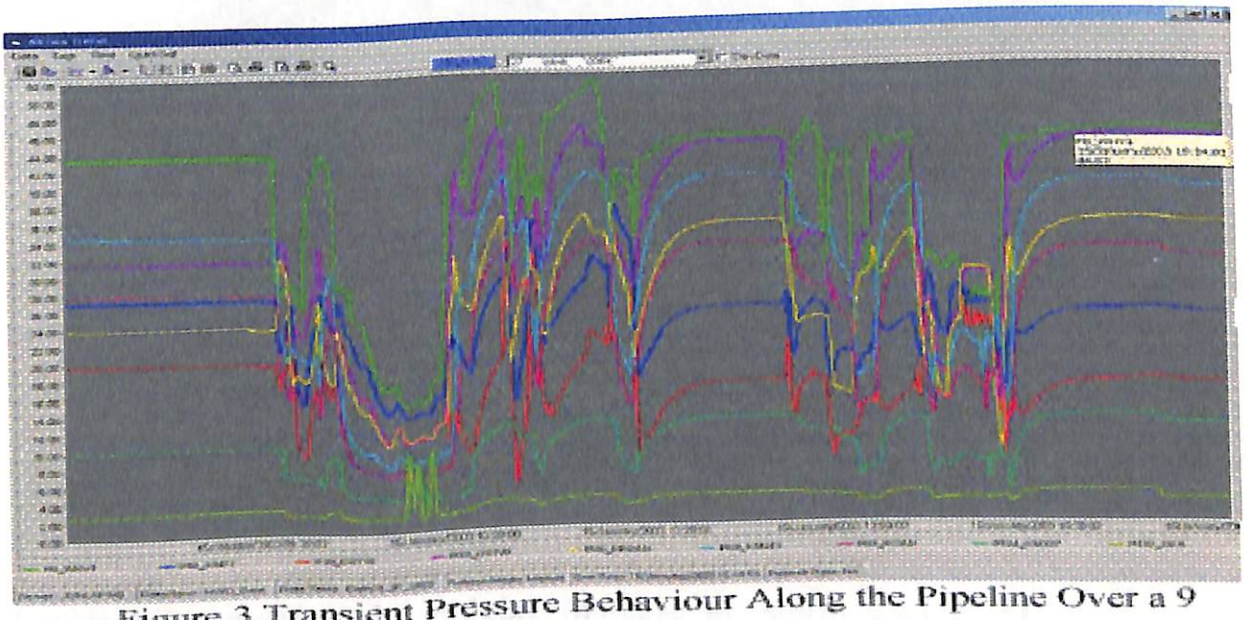

Figure 3 Transient Pressure Behaviour Along the Pipeline Over a 9 hour Period

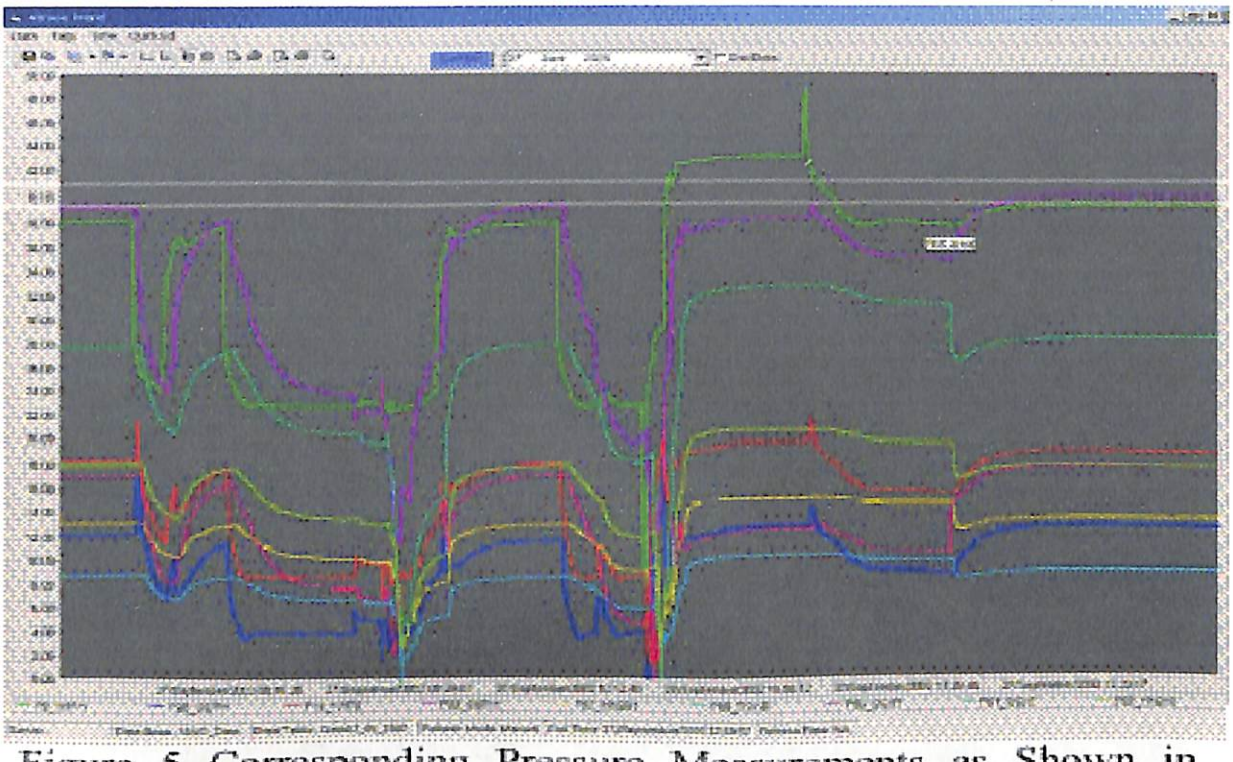

Figure 5 Corresponding Pressure Measurements as Shown in Figure 4 above

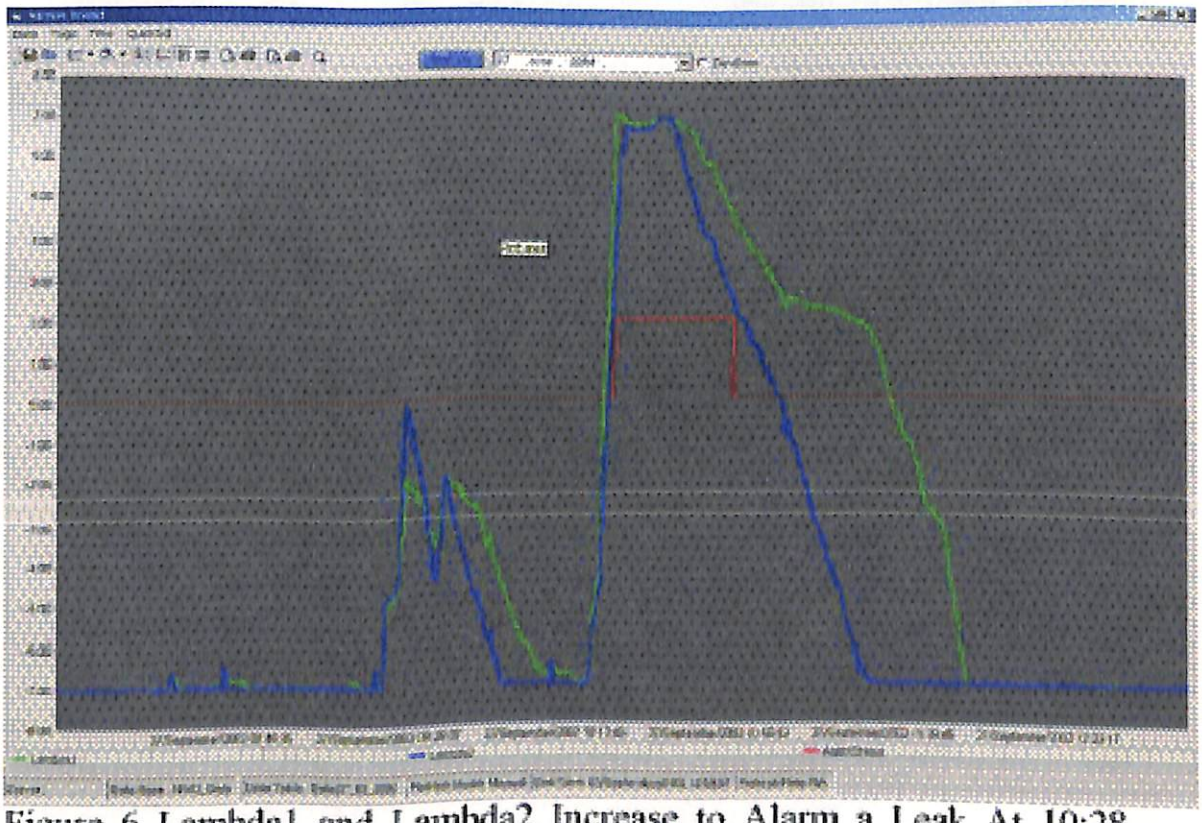

Figure 6 Lambda1 and Lambda2 Increase to Alarm a Leak At 10:28 hours (AlarmStatus Changes from 0 to 1, then 2). This is the same time window as shown in Fig. 4 and 5.

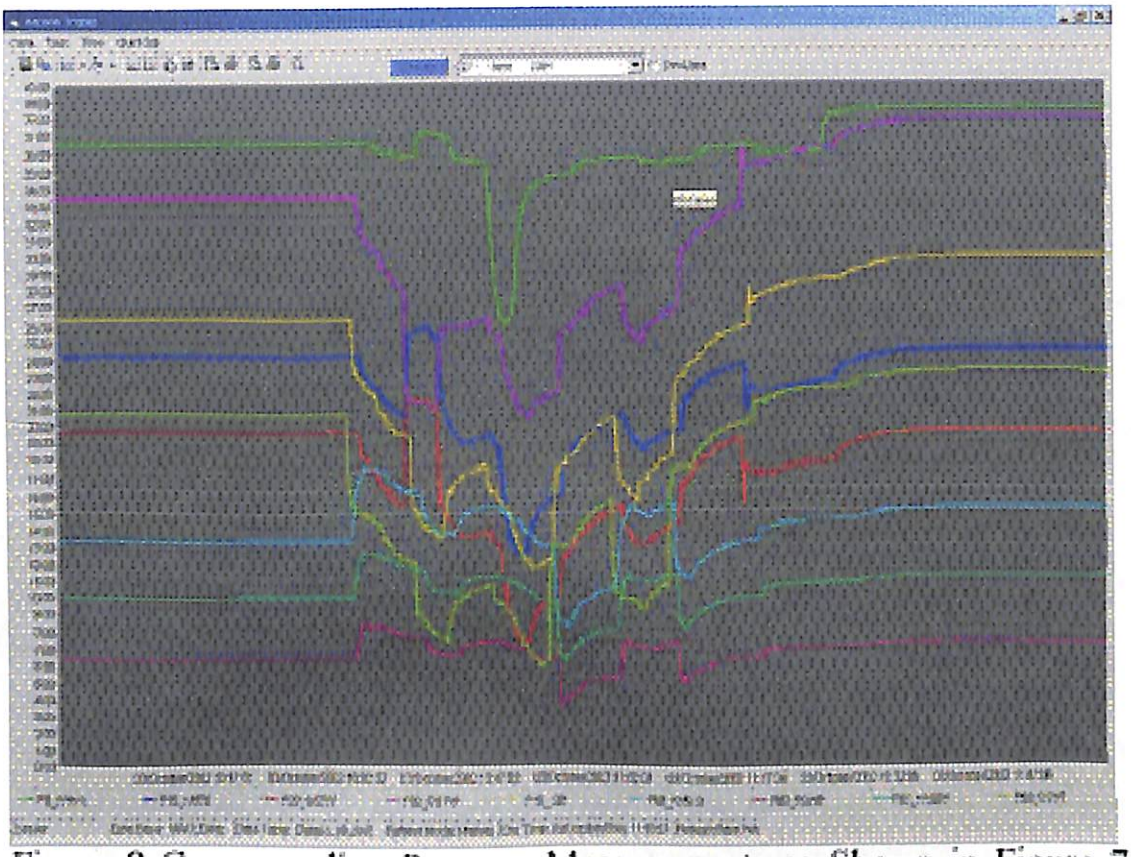

Figure 8 Corresponding Pressure Measurements as Shown in Figure 7 above

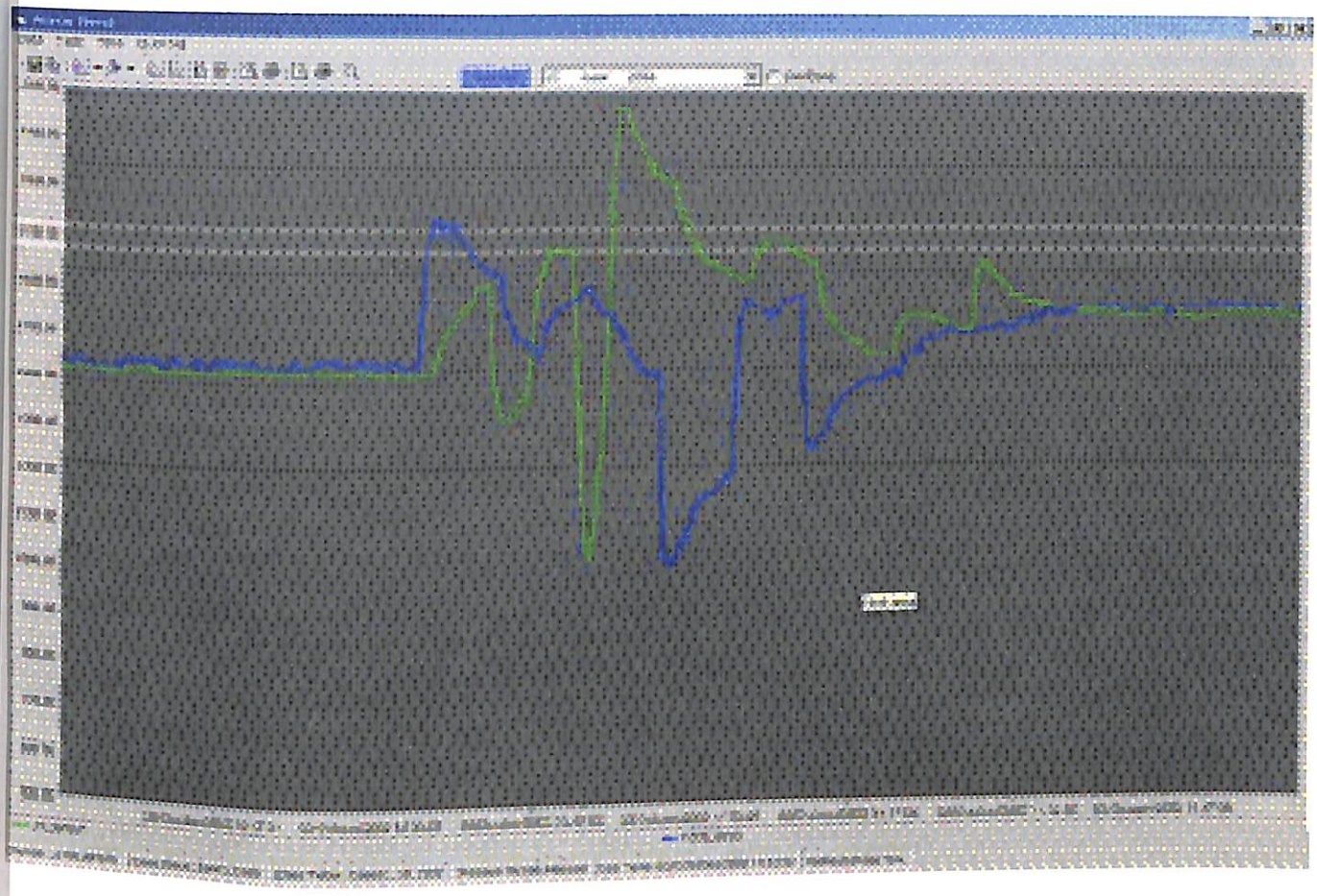

Figure 7 Flow Measurements Between 10 and 12 hours on 03/October/2002

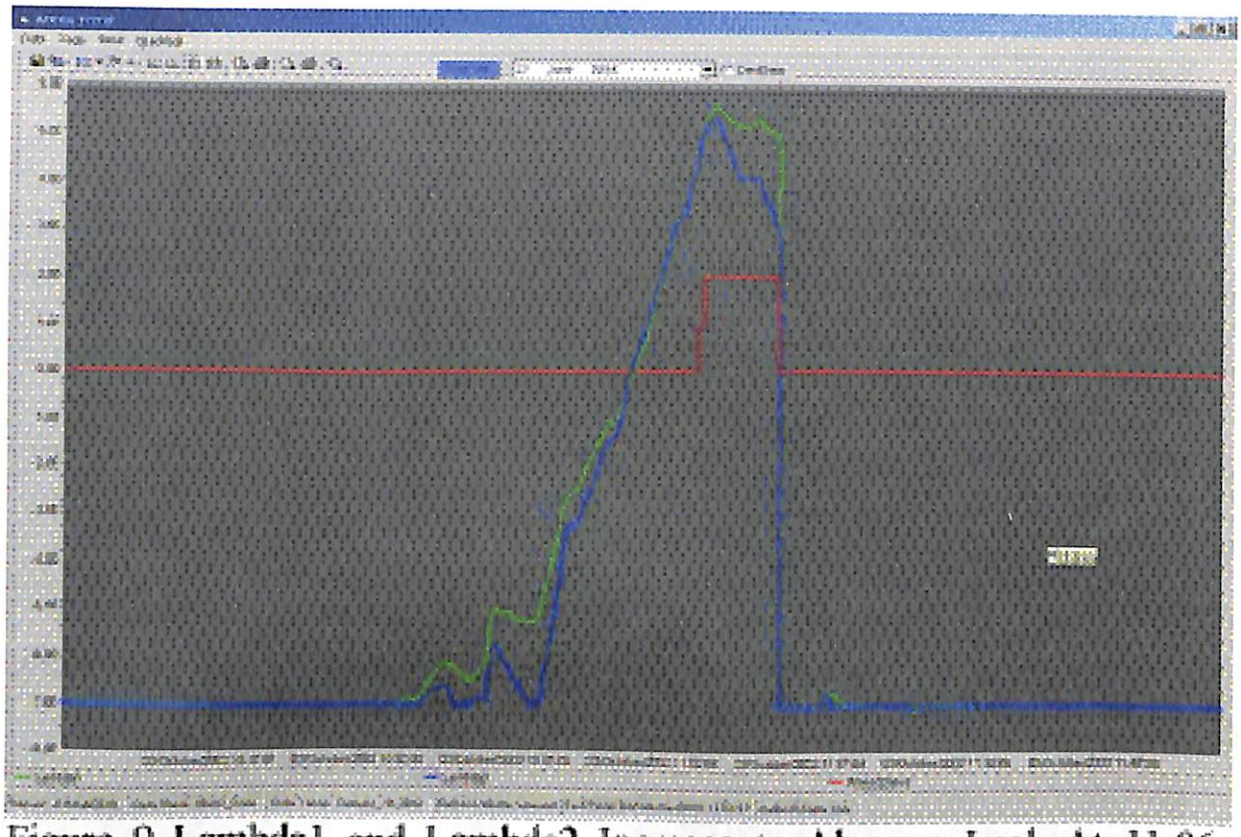

Figure 9 Lambda1 and Lambda2 Increase to Alarm a Leak At 11:06 hours (AlarmStatus Changes from 0 to 1, then 2)

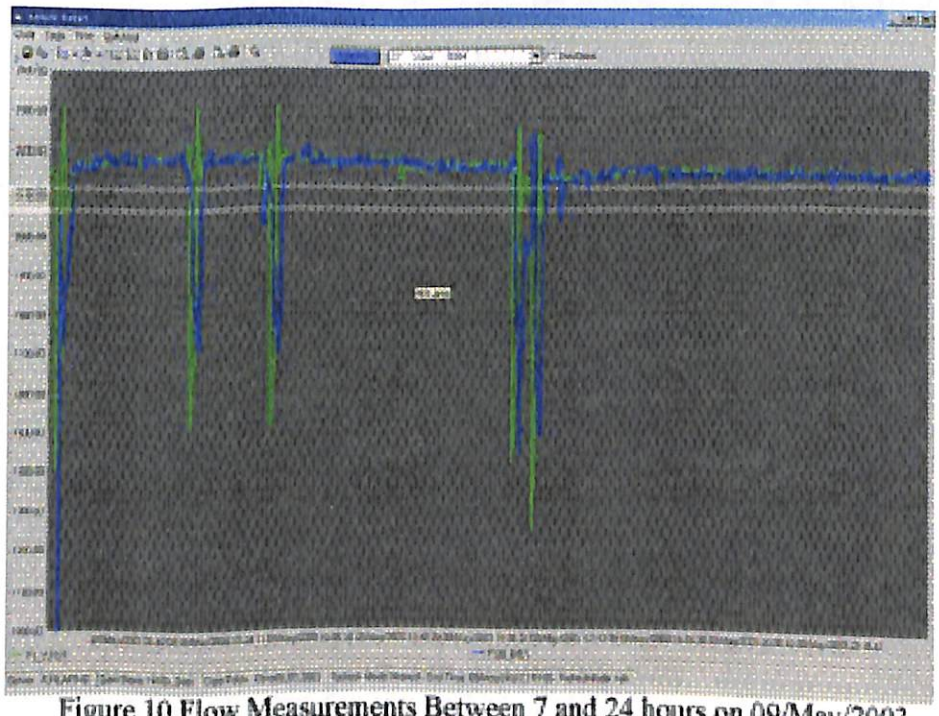

Figure 10 Flow Measurements Between 7 and 24 hours on 09/May/2003

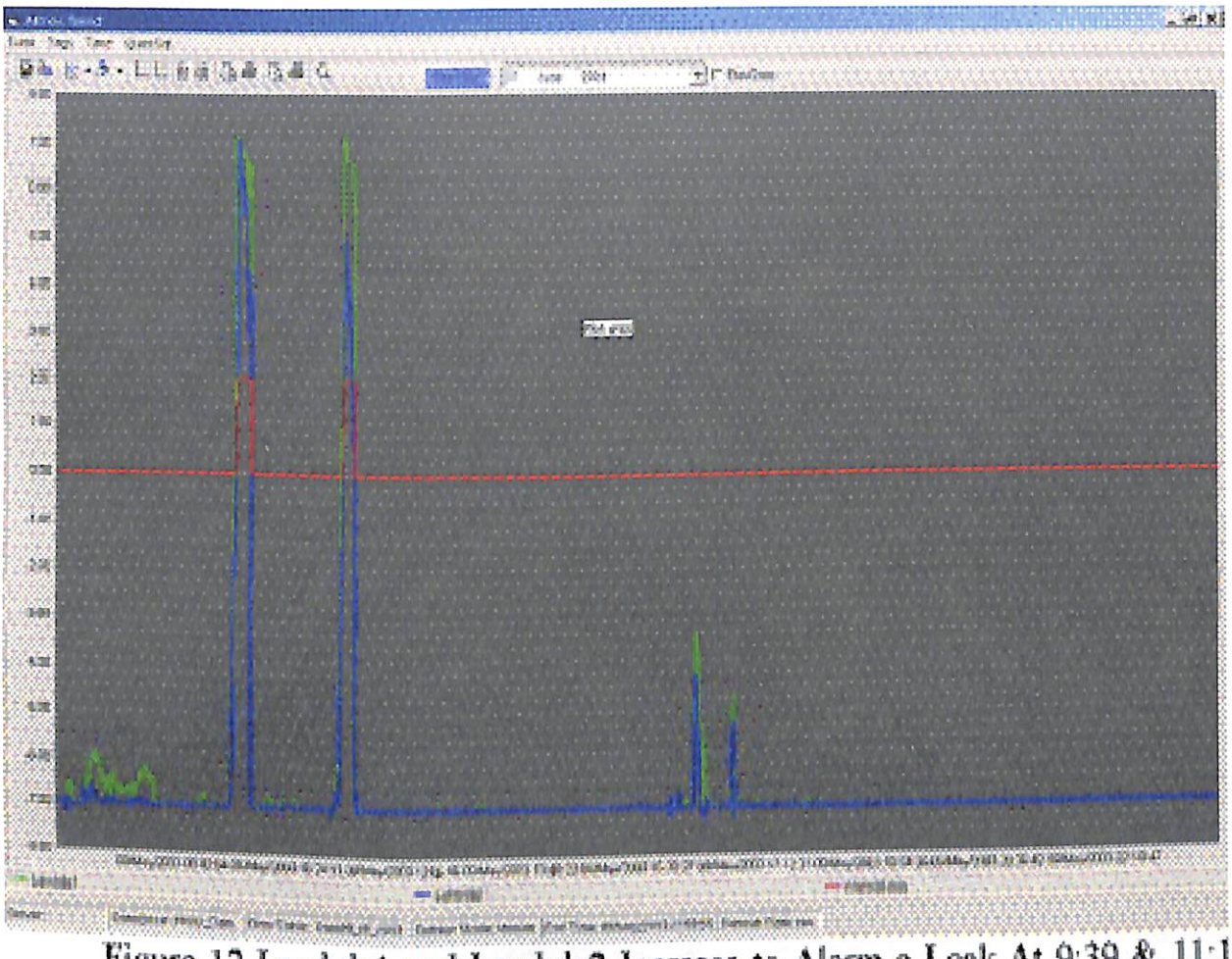

Figure 12 Lambda1 and Lambda2 Increase to Alarm a Leak At 9:39 & 11:14 hours (AlarmStatus Changes from 0 to 1, then 2)

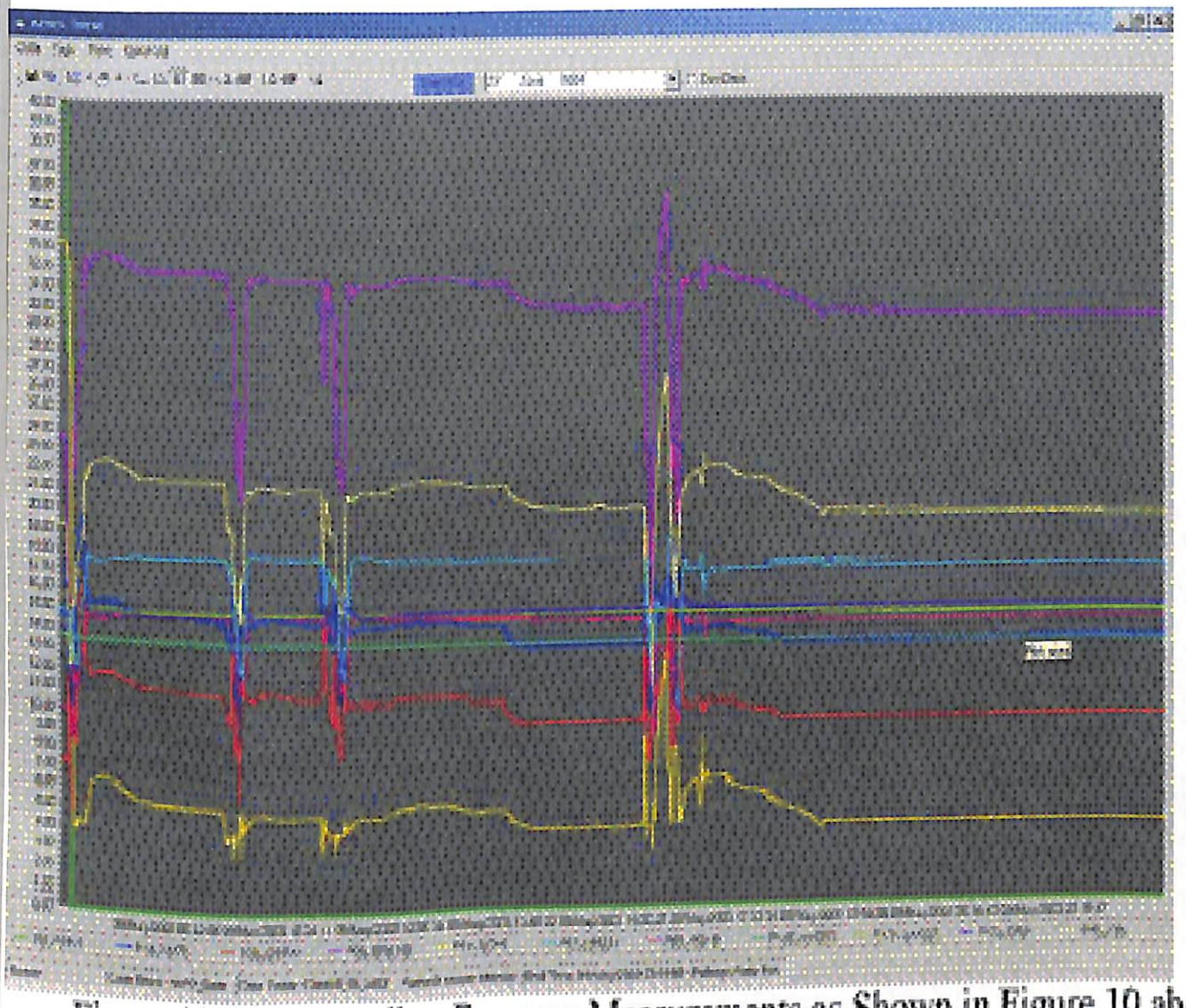

Figure 11 Corresponding Pressure Measurements as Shown in Figure 10 above

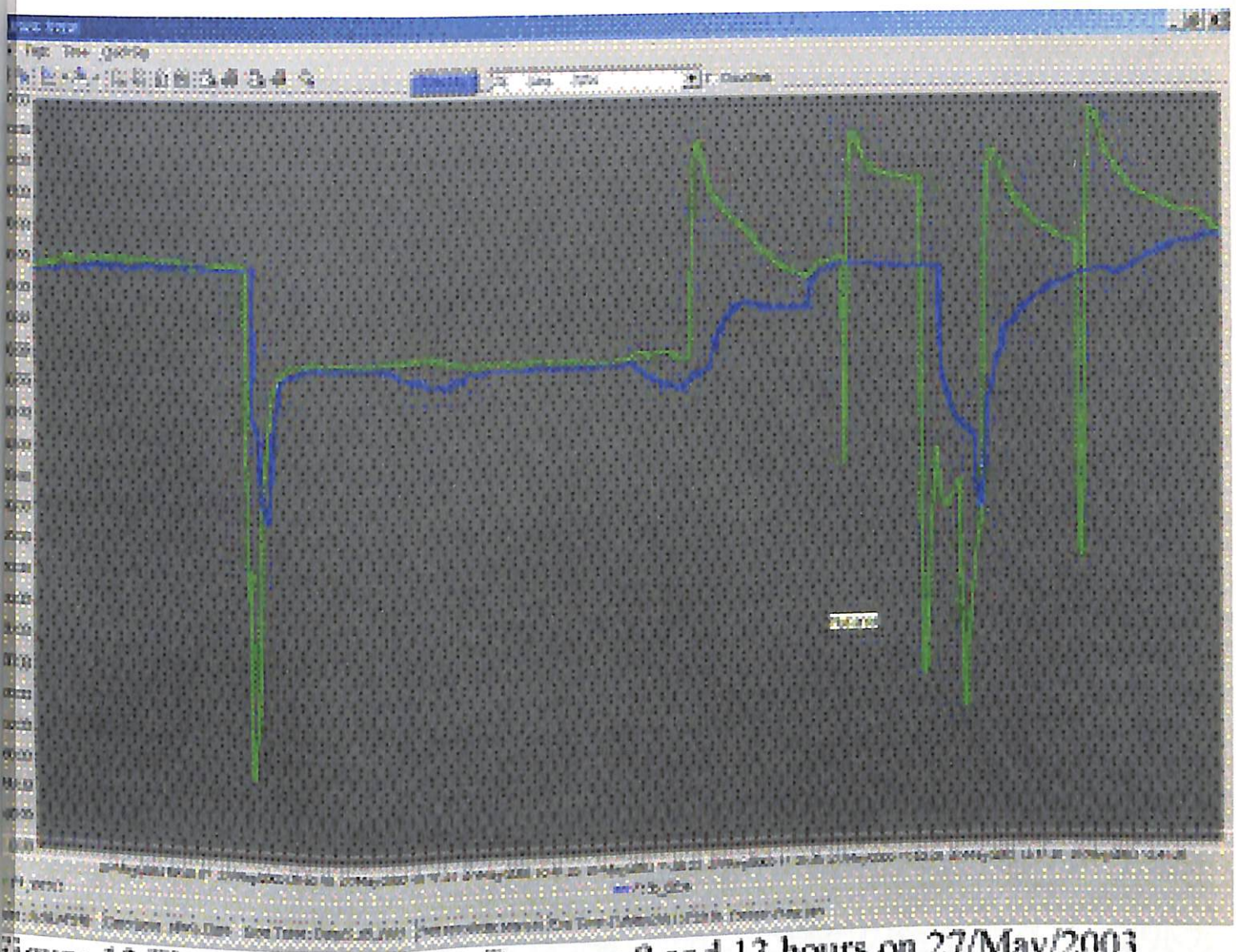

Figure 13 Flow Measurements Between 9 and 13 hours on 27/May/2003

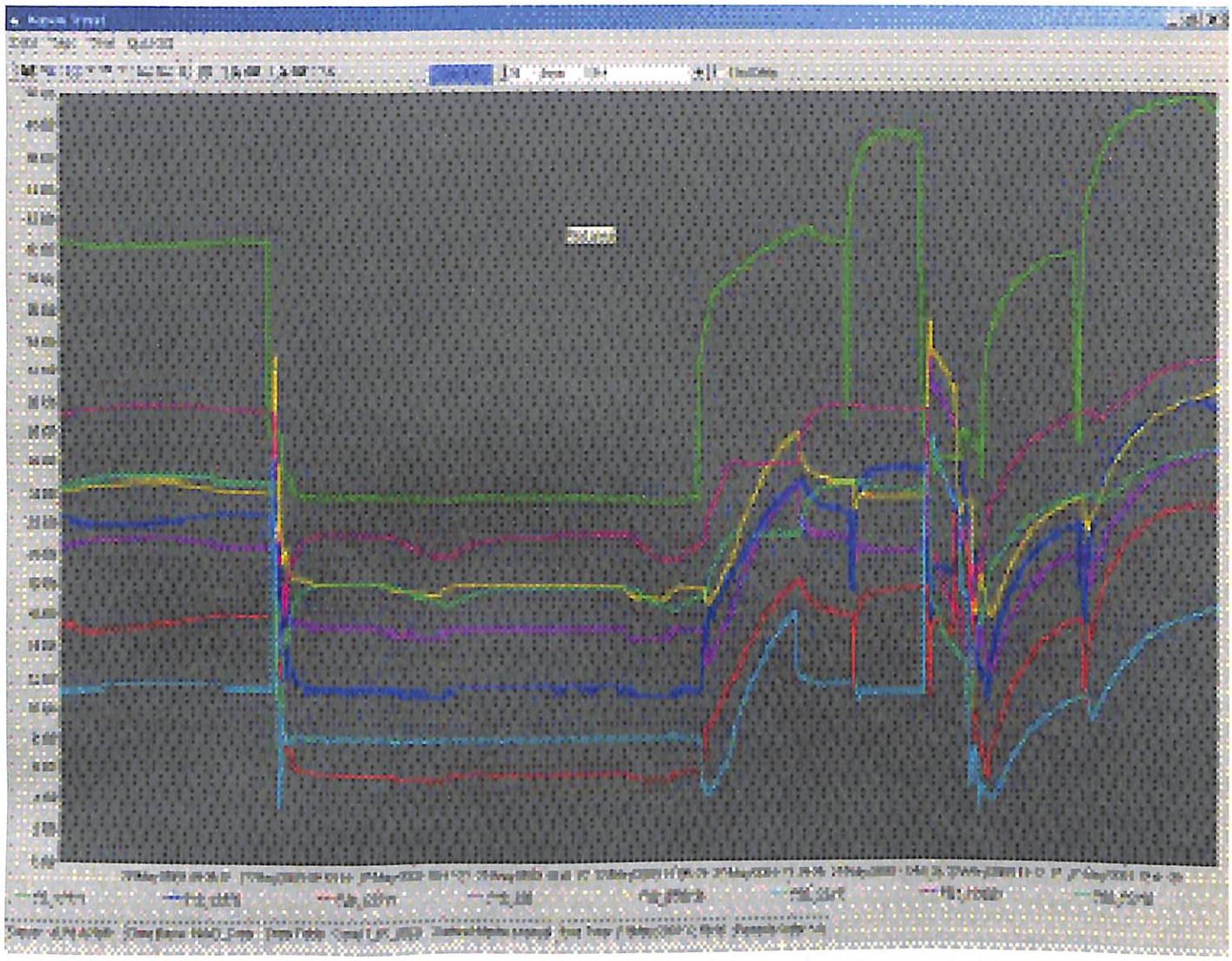

Figure 14 Corresponding Pressure Measurements as Shown in Figure 13 abo

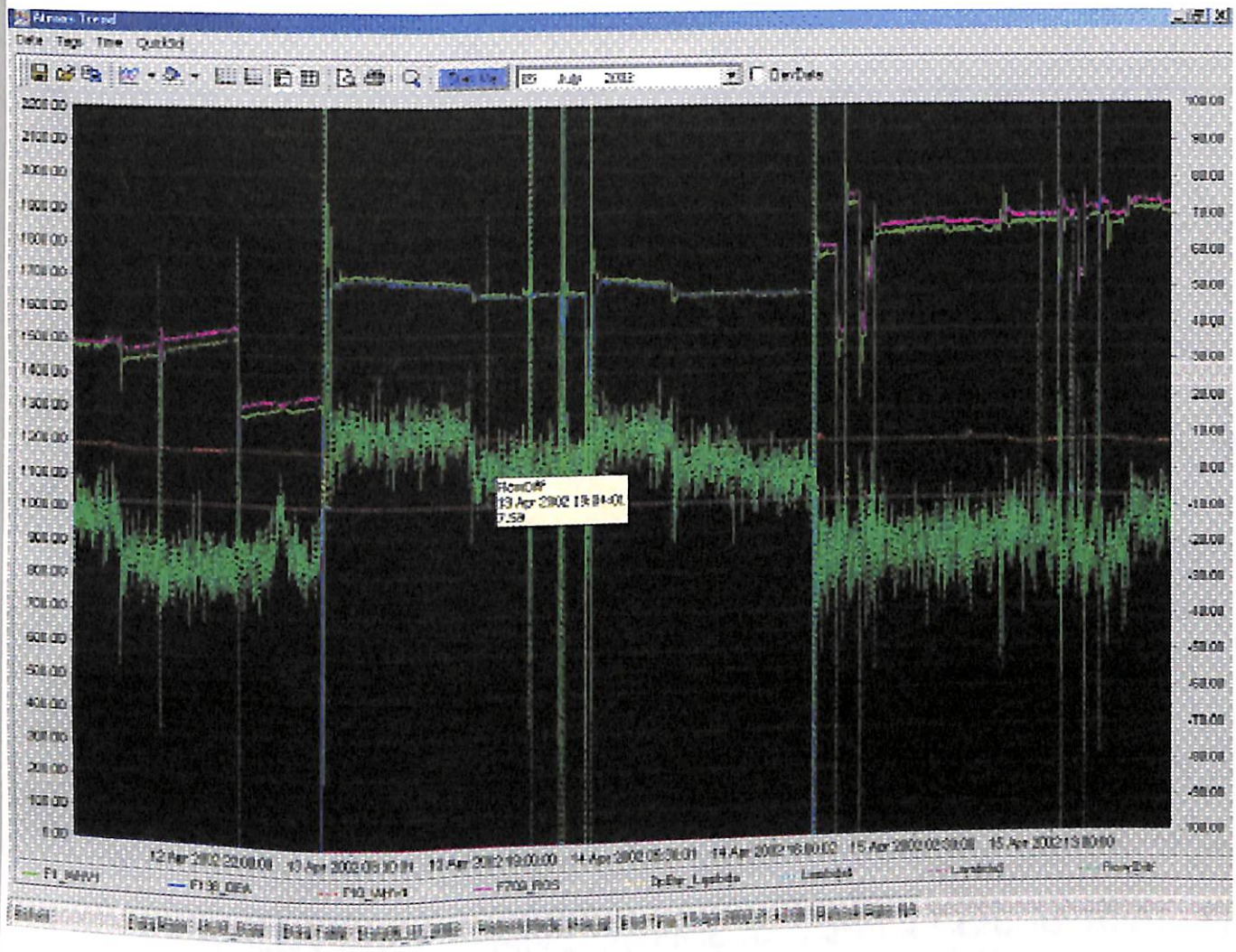

Figure 16 Flow Measurements and the Corresponding Flow Difference Under Steady-State Operating Conditions. Flow Difference (light green noisy line, scale on right hand axis) started at around −10 m^3/h at the start of the trend, it decreased to −20 when there was a small change in the flow-rate probably due to tank change. When the delivery changed from ROS (magenta line) to DEA (blue line), the flow difference increased from −20 to +10 m^3/h, and it decreased slightly during this transfer. When the delivery switched back to ROS, the flow difference went back to −20 m^3/h and it increased slightly before the end of the trend.

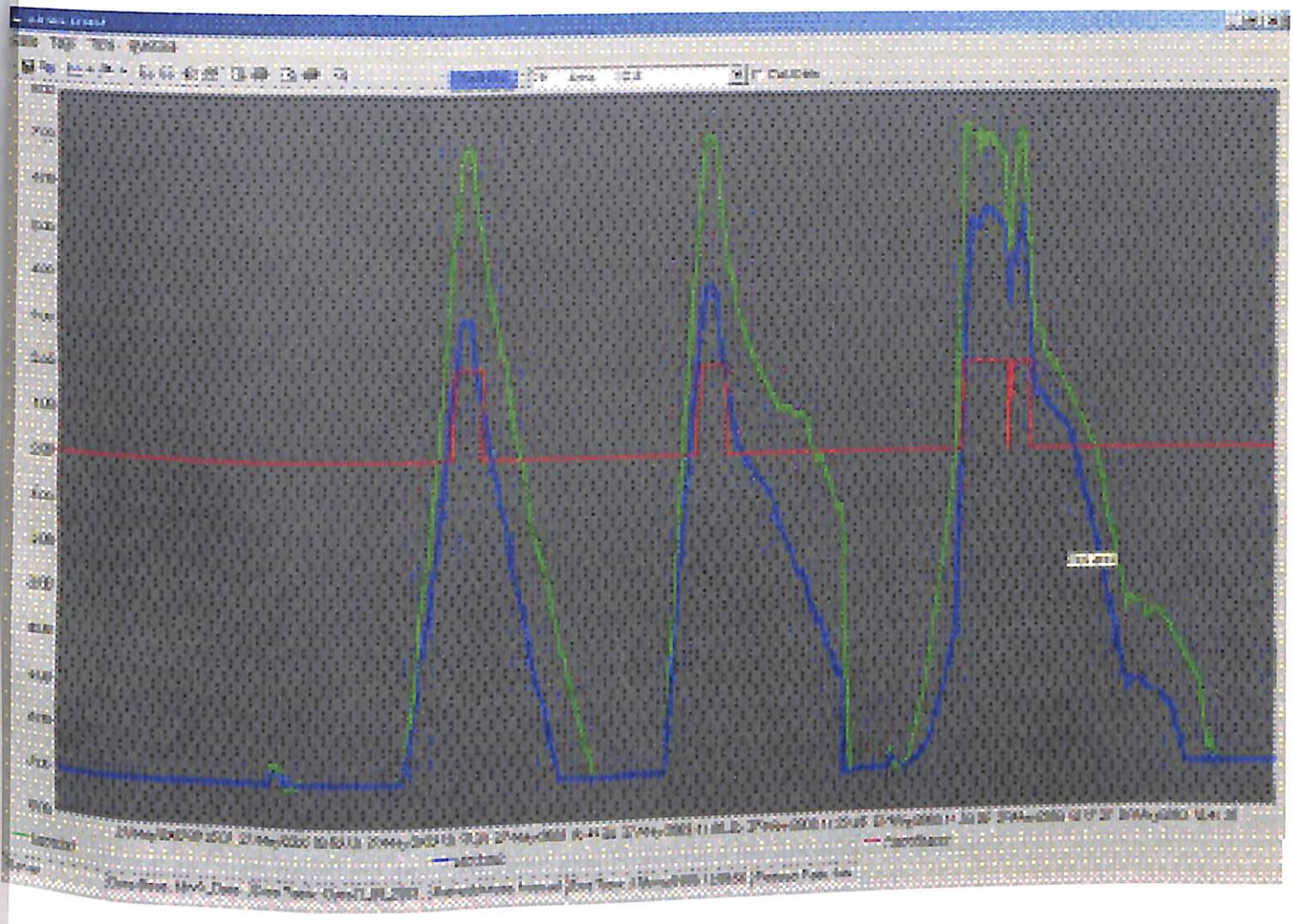

Figure 15 Lambda1 and Lambda2 Increase to Alarm a Leak At 10:21, 11:08 & 11:59 hours (AlarmStatus Changes from 0 to 1, then 2)

References

1. Norris, H.L. and D.W. Hissong: "Consequence Analysis in the Production and Transportation of Oil and Gas," SPE paper 27962 presented at the SPE/University of Tulsa Centennial Petroleum Engineering Symposium, Tulsa (August 29-31, 1994).

2. Norris, H.L. and R.C. Puls: "Single-Phase or Multiphase Blowdown of Vessels or Pipelines," SPE paper 26565 presented at the SPE Annual Meeting, Houston (October 3-6, 1993).

3. Kouba, G.E.: "A New Look at Measurement Uncertainty of Multiphase Flow Meters," ASME J. of Energy Resources Tech., 120, 56-60 (March 1998).

4. Mineral Management Service, "New Methods for Rapid Leak Detection in Offshore Pipelines" (April 1992).

5. Alaska Department of Environmental Conservation (1999), "Technical Review of Leak Detection Technologies Report"

6. Turner N.C., "Hardware and Software Techniques for Pipeline Integrity and Leak Detection Monitoring", SPE paper 23044 presented at the Offshore Europe Conference, Aberdeen (Sept. 3-6, 1991).

7. Zhang J., "Designing a Cost Effective and Reliable Pipeline Leak Detection System," Pipeline Reliability Conference, Houston (November 1996).

8. Website of Acoustic Systems Incorporated, http//: www.wavealert.com

9. E.Tapanes, "Fiber Optic Sensing Solutions for Real Time Pipeline Integrity Monitoring," Future Fibre Technologies Pty Ltd. Company Article.

10. Website of Tracer Research Corporation, http//: www.tracerresearch.com

11. Website of Controlotron, " http//: www.controlotron.com

12. "LASP Leak Alarm System for Pollutants" Teledyne Geotech, Garland, TX Marketing Information"

13. Website of Enviropipe, http//: www.enviropipe.com

14. Website of Simulutions Incorporated, http//: www.simulutions.com

15. Framer, E.J., " A New Approach to Pipe Line Leak Dectection," 1989 API Pipeline Conference, Dallas, Texas.

16. Farmer, E.J., Edwards,G., Wallis, D.F.., Byrom, J.A., and Kennedy, T.W., "Long-Term Field Tests Completed on Pipe Leak Detector Program, " Offshore August 1991.

17. Belsito, Salvatore, et al, "Leak Detection in Liquefied Gas Pipelines by Artificial Neural Networks", AICHE Journal, v44, Issue 12.

18. Nippon Kikai et al, "Neural Networks Implementation to Leak Localization Problems of Pipe Networks", Transactions of the Japan Society of Mechanical Engineers, Part C, v62, n595.

19. Mpesha, W " Leak Detection in Pipes by Frequency Response Method", Journal of Hydraulic Engineering, Feb 2001.

20. Aminian, K., "The Evaluation of Aerial Surveys for Detection of Natural Gas Pipeline Leaks", SPE 57461

21. Rence B, SPE 52679, "Aircraft-Mounted Forward-Looking Infrared Sensor System for Leak Detection, Spill Response and Wildlife Imaging on the North Slope of Alaska."

22. Jurdena Josep et al "Electrical Resistance Tomography to Detect Leak from Buried Pipes," Measurement Science and Technology, V2(8), Aug 2001.

23. Scott, S. L. and J. Yi, "Detection of Critical Flow Leaks in Deepwater Gas Flowlines," SPE paper 49310, proceedings of the SPE Fall Meeting, New Orleans (Sept. 1998); presented at the 1999 SPE/EPA Exploration and Production Environmental Conference, Austin Texas (Feb. 28 - March 3, 1999).

24. Scott, S.L., L. Liu and J. Yi: "Modeling the Effects of a Deepwater Leak on Behavior of a Multiphase Production Flowline," paper presented at the 1999 SPE/EPA E&P Environmental Conference, Austin Texas (Feb. 28 - March 3, 1999).

25. Dinis, J.M., A.J. Wojtanowicz and S.L. Scott: "Leak Detection in Subsea Flowlines with No Recorded Feed Rate," ASME J. of Energy Resources Tech., Vol. 121, 161-166 (Sept. 1999).

Appendix- A
OLGA Input File – Simulate Effect of Leak on Different Multiphase Flow Regimes

```
!
!*****************************************************************************
********
!- CASE Definition
!-----------------------------------------------------------------------------
CASE PROJECT="Exercise 1: Leak Detection", \
TITLE="Effect of leak on Reservoir/ Wellhead"
!
!*****************************************************************************
********
!- OPTIONS Definition
!-----------------------------------------------------------------------------
OPTIONS COMPOSITIONAL=OFF, DEBUG=OFF, PHASE=THREE,
POSTPROCESSOR=ON, SLUGVOID=SINTEF, STEADYSTATE=ON,
TEMPERATURE=WALL, \
WAXDEPOSITION=OFF
!
!*****************************************************************************
********
!- FILES Definition
!-----------------------------------------------------------------------------
FILES PVTFILE="deep_new.tab"
!
!*****************************************************************************
********
!- INTEGRATION Definition
!-----------------------------------------------------------------------------
INTEGRATION CPULIMIT=2 h, DTSTART=0.01 s, ENDTIME=0.5 h, MAXDT=5 s,
MAXTIME=0 s, MINDT=0.01 s, MINTIME=0 s, \
NSIMINFO=10, STARTTIME=0 s
!*****************************************************************************
********
! WATEROPTIONS Definition
!*****************************************************************************
********
WATEROPTIONS DISPERSIONVISC=ON, INVERSIONWATERFRAC=0.5 ,
WATERFLASH=ON, WATERSLIP=ON
!*****************************************************************************
********
!- MATERIAL Definition
!-----------------------------------------------------------------------------
MATERIAL LABEL=STEEL, CAPACITY=500 J/kg-C, CONDUCTIVITY=50 W/m-K,
DENSITY=7850 kg/m3, TYPE=SOLID
MATERIAL LABEL=INSULATION, CAPACITY=1500 J/kg-C,
CONDUCTIVITY=0.135 W/m-K, DENSITY=1000 kg/m3, TYPE=SOLID
```

```
MATERIAL LABEL=FORMATION, CAPACITY=1256 J/kg-C,
CONDUCTIVITY=1.59 W/m-K, DENSITY=2243 kg/m3, TYPE=SOLID
!
!*************************************************************************
********
!- WALL Definition
!-------------------------------------------------------------------
WALL LABEL=WALL-1, ELECTRICHEAT=OFF, MATERIAL=( STEEL,
INSULATION, INSULATION ), POWERCONTROL=OFF, THICKNESS=( 0.009, \
2:0.0125 ) m

WALL LABEL=WALL-2, ELECTRICHEAT=OFF, MATERIAL=( STEEL,
INSULATION, INSULATION ), POWERCONTROL=OFF, THICKNESS=( 0.0075, \
2:0.0125 ) m
WALL LABEL=WELL_WALL, ELECTRICHEAT=OFF, MATERIAL=( STEEL,
FORMATION, FORMATION, FORMATION, FORMATION ), \
POWERCONTROL=OFF, THICKNESS=( 0.00688, 4:0.15 ) m
GEOMETRY LABEL=FLOWLINE, XSTART=707 m, YSTART=0 m, ZSTART=0 m
PIPE LABEL=PIPE_1, DIAMETER=4 in, ELEVATION=0 m, LENGTH=1000 m,
NSEGMENTS=5, ROUGHNESS=2.8e-005 m, WALL=WALL-1
PIPE LABEL=PIPE_2, ELEVATION=5 m, LENGTH=400 m, NSEGMENTS=2
PIPE LABEL=PIPE_3, ELEVATION=-5 m, LENGTH=400 m, NSEGMENTS=2
PIPE LABEL=PIPE_4, ELEVATION=0 m, LENGTH=1600 m, NSEGMENTS=8
PIPE LABEL=PIPE_5, ELEVATION=-15 m, LENGTH=900 m, LSEGMENT=( 3:200,
150, 90, 60 ) m, NSEGMENTS=6
PIPE LABEL=PIPE_6, DIAMETER=0.1 m, ELEVATION=1524.0045963979 m,
LENGTH=1524.0045963979 m, NSEGMENTS=5, WALL=WALL-2
PIPE LABEL=PIPE_7, ELEVATION=0 m, LENGTH=120 m, NSEGMENTS=2
GEOMETRY LABEL=WELLBORE, XSTART=0 m, YSTART=-1507 m, ZSTART=0
m
PIPE LABEL=WELLBORE-1, DIAMETER=4 in, ELEVATION=707 m,
LENGTH=1000 m, NSEGMENTS=5, ROUGHNESS=2.5e-005 m, \
WALL=WELL_WALL
PIPE LABEL=WELLBORE-2, ELEVATION=800 m, LENGTH=800 m,
NSEGMENTS=4
!
!*************************************************************************
********
!- NODE Definition
!-------------------------------------------------------------------
NODE LABEL=PERFS, TYPE=TERMINAL, X=0 m, Y=0 m, Z=0 m
NODE LABEL=WELLHEAD, TYPE=MERGE, X=0 m, Y=0 m, Z=0 m
NODE LABEL=PLATFORM, TYPE=TERMINAL, X=0 m, Y=0 m, Z=0 m
BRANCH LABEL=WELLBORE, FLOAT=ON, FLUID="1", FROM=PERFS,
GEOMETRY=WELLBORE, TO=WELLHEAD
```

```
BRANCH LABEL=FLOWLINE, FLOAT=ON, FLUID="1", FROM=WELLHEAD,
GEOMETRY=FLOWLINE, TO=PLATFORM
!
!*****************************************************************
********
!- BOUNDARY Definition
!---------------------------------------------------------------
BOUNDARY NODE=PERFS, TYPE=CLOSED
BOUNDARY GASFRACTION=1 -, NODE=PLATFORM, PRESSURE=145.037 psia,
TEMPERATURE=22 C, TIME=0 s, TYPE=PRESSURE, \
WATERFRACTION=0 -
!
!*****************************************************************
********
!- HEATTRANSFER Definition
!---------------------------------------------------------------
HEATTRANSFER BRANCH=WELLBORE, HAMBIENT=6.5 W/m2-C,
HMININNERWALL=10 W/m2-C, HOUTEROPTION=HGIVEN, INTAMBIENT=68 C,
\
INTERPOLATION=VERTICAL, OUTTAMBIENT=6 C
HEATTRANSFER BRANCH=FLOWLINE, HAMBIENT=6.5 W/m2-C,
HMININNERWALL=10 W/m2-C, HOUTEROPTION=HGIVEN,
INTERPOLATION=SECTIONWISE, \
TAMBIENT=6 C
!*****************************************************************
********
! CONTROLLER Definition
!*****************************************************************
********
CONTROLLER LABEL=CONTROLLER-1, COMBINEVARIABLES=OFF,
EXTENDED=OFF, MAXCHANGE=0.2 , SETPOINT=( 0, 0.015625 ) , \
STROKETIME=33.33 s, TIME=( 0, 1 ) s, TYPE=MANUAL
!*****************************************************************
********
! SOURCE Definition
!*****************************************************************
********
SOURCE LABEL="WATER INGRESS", BRANCH=FLOWLINE, CD=0.84 ,
CONTROLLER=CONTROLLER-1, DIAMETER=0.5 in,
CRITFLOWMODEL=FROZEN, \
PIPE=PIPE_4, PRESSURE=2165 psia, SECTION=4, TEMPERATURE=8 C,
TOTALWATERFRACTION=1 -
!*****************************************************************
********
! WELL Definition
```

```
!*************************************************************************
********
WELL LABEL=WELLS, AINJ=0 , APROD=0 , BINJ=3e-006 , BPROD=3e-006 ,
BRANCH=WELLBORE, GASFRACTION=-1 -, \
INJOPTION=LINEAR, ISOTHERMAL=YES, LOCATION=MIDDLE,
PIPE=WELLBORE-1, PRODOPTION=LINEAR, RESPRESSURE=100 bara, \
RESTEMPERATURE=100 F, SECTION=1, TIME=0 s, WATERFRACTION=0 -,
WAXFRACTION=0 -
!*************************************************************************
********
! VALVE Definition
!*************************************************************************
********
VALVE LABEL=WH-VALVE, BRANCH=WELLBORE, CD=0.84 ,
CRITFLOWMODEL=FROZEN, DIAMETER=0.089 m, OPENING=1 ,
PIPE=WELLBORE-2, \
SECTIONBOUNDARY=5, TIME=0 s
VALVE LABEL=PF-VALVE, BRANCH=FLOWLINE, CD=0.84 ,
CRITFLOWMODEL=FROZEN, DIAMETER=0.12 m, OPENING=1 , PIPE=PIPE_7, \
SECTIONBOUNDARY=2, TIME=0 s
!
!*************************************************************************
********
!- PRINTINPUT Definition
!-------------------------------------------------------------------
PRINTINPUT KEYWORD=GEOMETRY
PRINTINPUT KEYWORD=TABLE
!
!*************************************************************************
********
!- OUTPUT Definition
!-------------------------------------------------------------------
OUTPUT COLUMNS=4, DELETEPREVIOUS=OFF, DTOUT=2 h
OUTPUT BRANCH=WELLBORE, COLUMNS=4, DELETEPREVIOUS=OFF,
VARIABLE=( UL, UG, UD, AL, PT, DPT, BE, GA, ID )
OUTPUT BRANCH=WELLBORE, COLUMNS=4, DELETEPREVIOUS=OFF,
VARIABLE=( RMTOT, BOU, MG, ML, MD, TM, DTM )
OUTPUT BRANCH=FLOWLINE, COLUMNS=4, DELETEPREVIOUS=OFF,
VARIABLE=( UL, UG, UD, AL, PT, DPT, BE, GA, ID )
OUTPUT BRANCH=FLOWLINE, COLUMNS=4, DELETEPREVIOUS=OFF,
VARIABLE=( RMTOT, BOU, MG, ML, MD, TM, DTM )



!*************************************************************************
********
```

```
! TREND Definition
!*************************************************************************
********
TREND BRANCH=WELLBORE, DELETEPREVIOUS=OFF, DTPLOT=25 s,
PIPE=WELLBORE-1, SECTION=2, TIME=0 s, VARIABLE=( PT, \
TM, QG, QLTHL, QLTWT )
TREND BRANCH=FLOWLINE, DELETEPREVIOUS=OFF, DTPLOT=25 s,
PIPE=PIPE_1, SECTION=1, TIME=0 s, VARIABLE=( PT, \
TM, ID, USG, USL, QLTWT, QLTHL, QG )
TREND BRANCH=FLOWLINE, DELETEPREVIOUS=OFF, DTPLOT=25 s,
PIPE=PIPE_3, SECTION=1, TIME=0 s, VARIABLE=( PT, \
TM, ID, USG, USL, QLTWT, QLTHL, QG )
TREND BRANCH=FLOWLINE, DELETEPREVIOUS=OFF, DTPLOT=25 s,
PIPE=PIPE_3, SECTION=1, TIME=0 s, VARIABLE=( PT, \
TM, ID, USG, USL, QLTWT, QLTHL, QG )
TREND BRANCH=FLOWLINE, DELETEPREVIOUS=OFF, DTPLOT=25 s,
PIPE=PIPE_4, SECTION=6, TIME=0 s, VARIABLE=( PT, \
TM, ID, USG, USL, QLTWT, QLTHL, QG )
TREND BRANCH=FLOWLINE, DELETEPREVIOUS=OFF, DTPLOT=25 s,
PIPE=PIPE_5, SECTION=1, TIME=0 s, VARIABLE=( PT, \
TM, ID, USG, USL, QLTWT, QLTHL, QG )
TREND BRANCH=FLOWLINE, DELETEPREVIOUS=OFF, DTPLOT=25 s,
PIPE=PIPE_4, SECTION=4, TIME=0 s, VARIABLE=( PT, \
TM, ID, USG, USL, QLTWT, QLTHL, QG )
TREND BRANCH=FLOWLINE, DELETEPREVIOUS=OFF, DTPLOT=25 s,
PIPE=PIPE_7, SECTION=1, TIME=0 s, VARIABLE=( PT, \
TM, ID, USG, USL, QLTWT, QLTHL, QG )
!
!*************************************************************************
********
!- PROFILE Definition
!-------------------------------------------------------------------------
PROFILE DELETEPREVIOUS=OFF, DTPLOT=0.25 h, VARIABLE=( HOL, TM, PT,
GT, ID )
PROFILE BRANCH=FLOWLINE, DELETEPREVIOUS=OFF, DTPLOT=0.25 h,
VARIABLE=( USG, USL )
!
ENDCASE
```